Capillary Underfill Manufacturing Development and Characterization for 2nd Level Electronic Interconnect Processes

By

Benjamín Salomón

A project submitted in partial fulfillment of the requirements for the degree of

MASTER OF ENGINEERING

in

MANAGEMENT SYSTEMS ENGINEERING

UNIVERSITY OF PUERTO RICO
MAYAGÜEZ CAMPUS
DECEMBER, 2004

Approved by:

_____   _____
María Irizarry, Ph. D.   Date
Member, Graduate Committee

_____   _____
David González, Ph.D.   Date
Member, Graduate Committee

_____   _____
Pedro Resto, Ph.D.   Date
President, Graduate Committee

_____   _____
Edgardo Lorenzo, Ph D.   Date
Graduate Studies Representative

_____   _____
Agustín Rullán, Ph.D.   Date
Chairperson of the Department

Ben Salomon

ABSTRACT

The work contained in this study establishes the process framework and methodology for implementing an underfill operation for an electronics manufacturing plant. The investigation explains development of the required process characterization, defines a range of equipment operability, recommends process/equipment parameters and methods, illustrates acceptability criteria and establishes the basis for future practical process development in this area.

This document may serve as a general technical reference manual (TRM) for the second level interconnect underfill process as developed for an electronic manufacturing plant. It includes complete process development for all operations related directly to the underfill operation such as underfill dispensing and underfill curing. The methodology presented here may be used as a tool for any future development of these processes or as a template for related underfill projects.

The findings in this study indicate that an underfill process while improving second level interconnect board reliability can have a negative impact on manufacturing imperatives by adding cost and overhead. A successful implementation of a cost effective underfill process requires a strong collaborative effort between product designer, manufacturing engineer, underfill and dispensing systems supplier.

RESUMEN

El estudio establece los procesos y metodologías para desarrollar la nueva tecnología de *underfill* para interconexiones de segundo plano (second level interconnect) en tarjetas de circuitos integrados. La investigación desglosa el desarrollo requerido para caracterizar los procesos de esta tecnología en una planta de ensamblaje de tarjetas de circuitos integrados, define un margen de operabilidad, recomienda parámetros de proceso, establece criterios de calidad y fundamenta un método para desarrollo futuro en esta área.

El proyecto incluye el desarrollo completo para todas la operaciones de underfill tanto para la operación de dispensado como la de curado. La metodología que se desarrolla establece una forma para enmarcar futuros proyectos relacionados a esta nueva tecnología en este tipo de industria.

El resultado de este proyecto indica que añadir una operación de *underfill* en una planta de manufactura de ensamblajes electrónicos puede tener un impacto negativo en términos de costo y en flujo de producto. Minimizar estos efectos conlleva una estrecha colaboración entre diseñador e ingeniero de manufactura. De la misma forma, el diseño del proceso de *underfill* requiere que los materiales y equipos se ajusten a los requerimientos para cada producto. La decisión de implantar este proceso como una operación más en la manufactura de tarjetas de circuitos integrados se decide solamente después de sopesar los beneficios en confiabilidad y los costos incrementales inherentes a un proceso de dispensado *underfill*.

ACKNOWLEDGEMENTS

To Carmen, Coral and Javier, thank you for your patience and your support. My love to you always.

Special thanks to Pedro, David, Sonia, Viviana and Anaida for their encouragement, support and for believing in me.

To the Professors and Administration in the IE department I express my gratitude for allowing me the opportunity to further my education. Your professionalism has inspired me to go the extra mile.

Last but not least, my love to my parents and all family, immediate and extended, as always. God Bless all of you.

TABLE OF CONTENTS

LIST OF FIGURES

LIST OF TABLES

1   INTRODUCTION

This section presents the project's objective and general background project information

1.1   Objective

The purpose of this project is to investigate and establish the required methods and processes required for implementing an underfill operation for an electronics manufacturing plant. This document may serve as a general technical reference manual (TRM) for implementing the second level interconnect underfill process for array components such as chip scale array (CSP) packages and ball grid array (BGA) components. It includes complete process development for all processes related directly to the underfill operation such as underfill dispensing and underfill curing. The methodology presented here may be used as a tool for any future development of these processes or as a template for related underfill projects.

1.2   Background

A variety of present day industry packaging trends are affecting board-level reliability. The reduction in chip size, the expanding market of portable consumer electronics, and the critical application of some equipment in the military aerospace industry are some reasons why improved product reliability in the electronic industry is required. The widely expanding use of solder bumped area array packages in these demanding applications has driven change across many of the fundamental processes used in the electronics manufacturing industry.

While the size of electronic components has been decreasing, the number of input/output (I/O) terminations has been increasing. As postulated by Moore's law, the trend in the number of transistors per integrated circuit has grown exponentially for the

last 40 years. A graphical representation of this effect over the last three decades is represented in Figure 1. As a direct result of this overcrowding and miniaturization, the density of solder joint connections has increased while overall package dimensions have decreased. Furthermore, there is a strong tendency to design with smaller solder joints and larger die to substrate ratios as the need increases for packages with more performance options. In today's packaging technology, area array packages, such as Ball Grid Array packages (BGA) have become prevalent due to package performance, manufacturing yield and pin count.

Crucial to long term reliability of electronic packages is the understanding of solder joint failure modes during thermal cycling. Repeated thermal cycling can cause expansion and contraction of the materials used in printed circuit board (PCB) assemblies. Thermally induced stresses are created when the rate of this expansion and contraction between board and component is significantly different. As an example, (Figure 2) most chips have a coefficient of thermal expansion (CTE) of 2 parts per million per degree Centigrade (ppm/ºC), while PCB CTE's are in the range of 15-25 ppm/°C. This CTE mismatch stresses the solder joints (the solder balls soldered to the PCB) of array packages and these stresses lead to circuit failures.
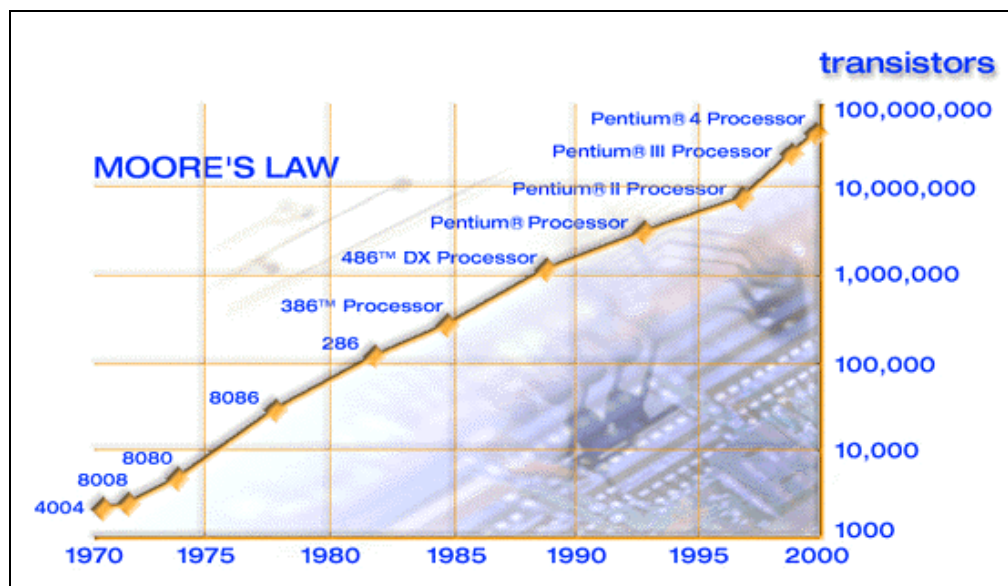
Figure 1: Validation of Moore's Law since 1970

Ben Salomon

Shear stresses caused by the CTE difference between component and printed circuit board is a primary cause of array type package solder joint failures [21]. The study presented here will focus on the application of capillary underfills for ball grid array packages. The proposed methods and processes, however, may be applied to a wide range of other components with solder ball array packaging such as chip scale packages (CSP).

Material	CTE (ppm/°C)
Silicon Die	2.8
Eutectic solder ball (63Sn/37Pb) 2nd level interconnect	25
Solder Mask (SM)	95
Substrate	xy: 12.4 z: 57
Cu Pad	17.7
PCB	xy: 17.6 z:57
Mold Compound (MC)	xy:8 z: 32
Die Attach (DA) 1st level interconnect	xy:72 z:145
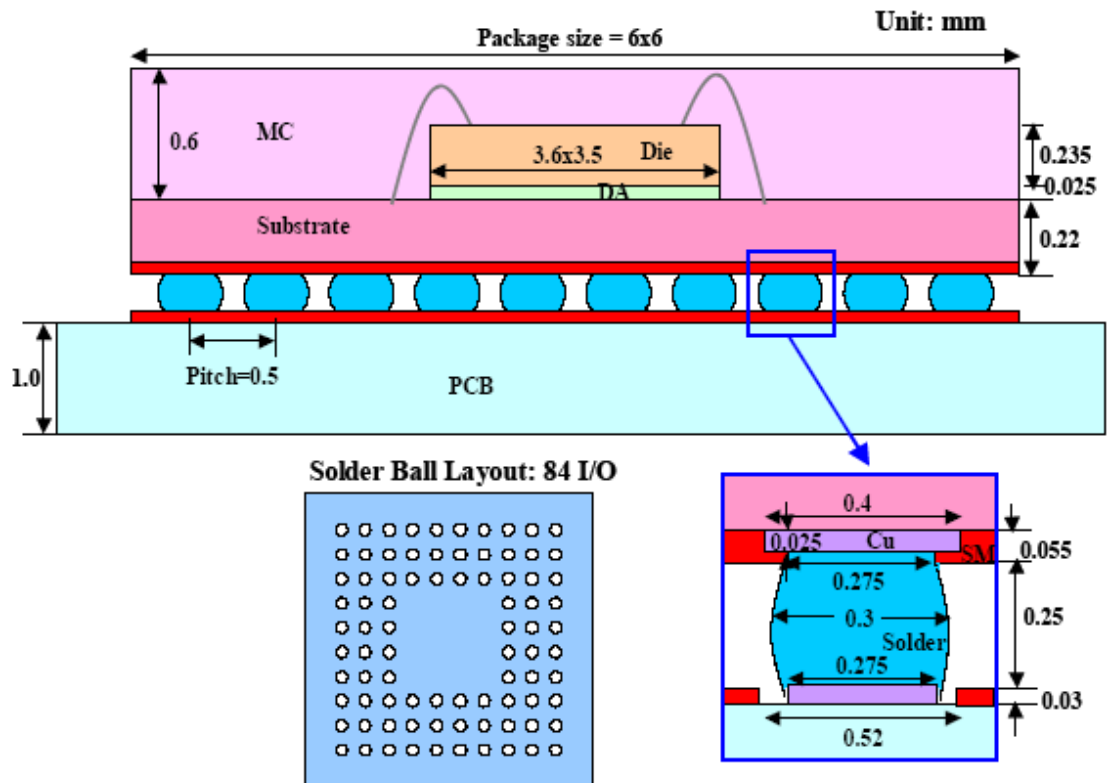
Figure 2 Physical Characteristics of a BGA Component [21]

Ben Salomon

A variety of techniques are available for increasing the board level reliability of BGA's. Among these are low expansion PCB's for ceramic BGA (CBGA) packages, interposers (buffers), between the component and PCB, repackaging or redesigning of the device. Using underfill to provide a layer between the BGA and PCB in order to reduce the strain on solder joints is another method. Underfill, while acting as a strain buffer between board and component, is a quick method of integrating high density chip-level designs with ever demanding board-level assembly constraints. Underfill however, by redistributing stresses and strains may create new ones within the device may not always perform as intended. Any underfill implementation scheme must be validated by thorough reliability life cycle tests.

Larger BGA's are capable of surviving commercial thermal cycling requirements without being underfilled. Greater separation of the BGA from the PCB (standoff height) reduces the shear strain induced during thermal cycling and a thicker substrate improves the fatigue life by increasing the mean CTE of the package, resulting in smaller CTE mismatch with the board.

The trend however in conventional processor packaging solutions is toward the design of smaller packages and rapid development cycles in order to satisfy the demands for further miniaturization of integrated circuits devices. Consumer demand for smaller and light weight portable electronic products like hand-phones, PDA's, digital cameras, and laptops are some examples that are driving the industry today. As electronic components move to smaller and thinner packages, the risk of these components to fail from thermally induced strains as shown in Figure 3, between the component and the PCB has the net effect of reducing fatigue life. Underfill reduces the CTE mismatch by encapsulating the BGA solder balls and redistributing the stress on these solder joints over a wider area.

An underfill is a composite material made up of an *epoxy polymer* with significant amounts of filler (silica added to the polymer to increase modulus and reduce CTE).

Additional components added to the underfill formulation are flow agents, adhesion promoters and dyes. Primarily used as the interface between die and substrate during component fabrication, underfill can also be placed under ball grid arrays (BGA) and chip scale packages (CSP). Some of the reasons underfill is used are:

1. Reducing the CTE mismatch between different materials as explained above.

2. Mechanical stability for extremely small components soldered to a PCB.

3. Moisture control. A properly chosen underfill will protect the component from environmental substances by sealing the interconnect area.

4. Protection from shock and vibration. Underfill can effectively reduce loads acting as a mechanical damper.

Underfill epoxies may be classified into four major groups:

1. **Capillary – material covered in this project.**
2. **Fluxing (No-Flow) - not used for 2nd level interconnect applications, not covered in this project.**
3. **Removable (Repairable) – repairable underfill, not covered in this project.**
4. **Corner Bond – underfill placed only at the corners of the component, not covered in this project.**

This classification is based on application and is currently changing as new materials and processes are being developed. Although this project focuses mainly on the process development and methodology for developing a capillary underfill process for BGA application, the manufacturing approach and general process development can be applied to similar components and materials that may demand a 2nd level interconnect underfill application. Even though the differences in technologies for each underfill type are significant, the general approach presented in this study can be applied with some modification and consideration for the material being used for each particular case. Removable underfill for example may require additional process development for repair, or corner bond material may demand less storage requirements and equipment. Even with these distinctions, the process template suggested by this study may serve as a development tool and reference.
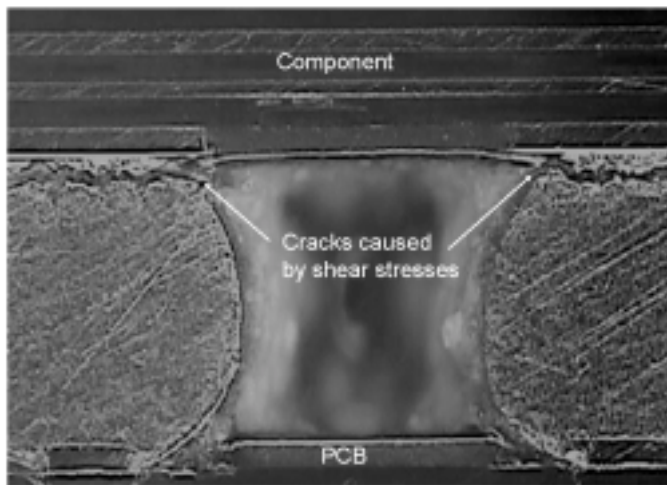
Figure 3: Cross Sectional View of Cracked BGA Solder Joints without underfill

1.2.1 Capillary underfill

Capillary underfills are low viscosity liquids designed to flow under a component by capillary action, wetting (adhering) to the component and board surfaces and encapsulating the solder joints. Underfill is applied close to the edge of the component to enable capillary forces to flood the gap between the component and the board. To do this, the underfill material must have a low viscosity, and the board is often heated to 70-100°C to aid the flow. Following dispensing, the underfill must then be cured. Although there are many different cure schedules, a typical cure schedule for quick-cure underfill is between fifteen to twenty minutes at 165°C. Conventional underfills are dispensed with a thin needle three mils or less from the edge of the chip surface of the board (Figure 4).
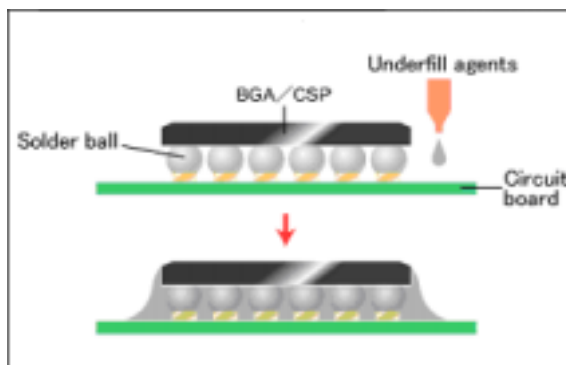
Figure 4: Schematic of a Capillary underfill Application

Ben Salomon

Low viscosity and excellent adhesion are both needed to promote rapid, complete encapsulation of solder joints and other features under the component. Dispensing of capillary underfill materials requires specialized equipment to achieve the accuracy and precision required for tight deposition control. Among other items, the dispenser must consistently repeat a dispensing pattern and apply a predetermined volume of underfill at the edge of the component. Heating the board and component is a common secondary requirement that improves wetting and accelerates capillary flow. Curing of the underfill is usually accomplished in reflow or dedicated curing ovens. Good capillary underfills are capable of flowing completely under a component and form "self-filleting" fillets. Climbing 50 to 100% up the component side with minimum "spilling" onto adjacent areas is generally recognized as a "good" fillet, of excellent reliability. Underfills that do not wet as well require a wide fillet before reaching sufficiently up the die edge. Inadequate fillets are more likely to crack and allow delamination around the fillet area.

1.2.2   Reworkable Underfill

Capillary underfills cannot be reworked or repaired during manufacture or in-field service, a fact that limits the widespread use of capillary underfill processes. Rework may be required for PCB's with components that fail during a final test or are returned from the field. Many such electronic devices contain PCBs that are too expensive to scrap because a single bad component cannot be repaired. Reworkable underfills allow underfilled components to be reworked and replaced. Chemically different from capillary underfill materials, reworkable underfills are designed to break down at high (rework) temperatures.

The rework process can actually be generally divided into three parts consisting of removal, cleaning and replacement. After cleaning, a new package can be attached to the board and underfilled. Tests have shown that reworkable underfill materials exhibit reliability comparable to that of traditional underfills. Reworkable underfills may have a

greater cost impact than capillary underfills and used only on boards that are not constrained to a limited number of thermal excursions (repairs).

1.2.3 Corner Bond Underfill

Corner bond underfill is currently being marketed as a viable underfill alternative for various applications and owes its development to the manufacturing limitations presented by traditional capillary underfills. Corner bond technology uses dots of adhesive that are typically applied at the corners of the component, where induced stresses are normally the greatest. This type of underfill can be applied using standard surface mount technology (SMT) dispense equipment, and cured during the solder reflow cycle. This speeds assembly and reduces costs by eliminating dedicated underfill dispense machines and cure ovens. As the epoxy is reworkable, it allows for the replacement of defective chips, and minimizes incidents where the entire board must be scrapped. The adhesive bond breaks down at temperatures exceeding 220ºC, allowing for relatively easy removal of the dots and replacement of the component.

An advantage often overlooked is the long term cost benefits of using corner bond material over traditional capillary underfill. Since corner bond is dispensed by dots at the corners of each component, consumption is a small fraction of what capillary underfill material would require by filling the volume under a component. In high volume operations, this cost is significant.

Corner bond underfill technology is limited by the height and geometry of the component. Since this material is added immediately after stencil printing, care must be taken to ensure that the epoxy does not touch the component's solder paste and that sufficient dot volume to bridge the gap between board and component is dispensed. Not all BGA's or CSP's are good candidates for corner bond underfill. Components using corner bond technology require a design that will allow enough space for dot placement without compromising paste deposition. Finally, corner bond underfill may simply not meet reliability goals for some components.

Ben Salomon

2   LITERATURE REVIEW

Macroscopic assessments of 2nd level interconnect underfill processes and operations from a manufacturing perspective have not been sufficiently addressed.   Individual contributors and industry sponsored literature in the field of underfill technology have focused on reliability, thermal evaluations of underfill packages, finite element analysis, product comparisons or specific and particular manufacturing concerns. The impact of 2nd level interconnect underfill applications on board level reliability has been given considerable attention, given the proliferation of BGA/CSP packages and new underfill materials.   Little attention has been given to the manufacturing development of this application on a practical level.   Criteria and acceptability standards for every day production processes are lacking. This project hopes to address this area and provide a method for future development in this area.

Schneider [1] discusses a procedure for capillary underfill deposition and documents improved board reliability with results from drop, thermal shock and humidity tests for different package geometries and different underfill materials. The procedure's process parameters are typical for an underfill operation. Failure mechanisms beyond the stipulated 1000 thermal cycles were found to be caused by solder fatigue near the interposer of the BGA/CSP package, confirmed, by FEA simulation. Other failures were induced during drop tests by combination of package geometry and underfill material. Schneider goes on to recommend a particular underfill having passed all tests and mentions this material for high reliability applications. Furthermore, the focus on fast processing, moderate storage conditions and optional rework qualities besides increased reliability are developments that drive the industry to develop these new materials.

Schneider [2] again in a related paper with the same data, discusses practical guidelines for CSP/BGA 2nd level interconnect underfill material with greater emphasis placed on best operational practices for a high volume manufacturing environment. The

Ben Salomon

paper discusses in greater detail the manufacturing and rework facet of the underfill process and establishes criteria for underfill selection. Criteria for underfill selection were based on manufacturing as well as design concerns. This is the only literature found that discusses the planning and implementation of an underfill strategy to some degree. The remaining part of the paper is similar or identical to the previous literature by Schneider mentioned above.

Doba [3], mentions current underfill materials for CSP and BGA packages, and compares reworkable and non-reworkable (capillary) underfill materials in a production environment. Doba's short paper extols the virtues of low temperature cure underfill epoxies that are reworkable and popular in Asia. These underfill materials, he implies, are suited for high volume operations with a minimum of overhead and processing.

A study documented by Haiwei Peng et al [4], presents a segment of the overall underfill development process and describes assembly and rework operations in some detail. In addition, results of reliability tests in this study strongly indicate significant mechanical improvement by implementing either reworkable or traditional capillary underfill. The rework process is reported not to degrade mechanical performance while underfill did not significantly alter thermal shock performance. Reliability improvements were reported to be nominally identical for both reworkable and non-reworkable materials.

Corner bond applications have hardly received any attention besides the usual industry sponsored promotional literature. The lack of peer reviewed literature in this area can be attributedted to the short time this technology has been on the market. One exception is a paper by Toleno and Schneider [5], working for Loctite Corporation, which discusses processing and reliability of corner bonded CSP's. Processing parameters such as dot dispensing characterization, maximum displacement effects and optimum dot placement are discussed in detail. The other half of the paper reviews the reliability performance of the corner bond material in comparison with several traditional underfills. Toleno and

Schneider reported results of drop tests and thermal cycling (-55ºC to 125ºC) on a wide range of component geometry and construction. Corner bond material was found to improve reliability in drop tests and thermal cycling for all components but the largest package (17 x 17 mm). The study also states minimal manufacturing impact by using this type of material. This last observation is important since the implementation of corner bond underfill is indeed the least disruptive on the production floor. Corner bond material can use typical glue dispensing equipment after stencil printing and deposit dots alongside solder paste prior to reflow. This is an advantage over traditional underfill processes where offline dispensing and a separate curing oven are required. Another mentioned advantage of corner bond underfill is the fact that this material can be reworked.

Pyland et al [6] discusses reliability issues by comparison of non-linear finite element analysis of underfilled and non-underfilled models. Interestingly, the study concludes that underfill may actually decrease solder joint reliability in some particular cases. Specifically, the conclusion reached by these investigators is that the underfill physical properties for large BGA components are critical in overall solder joint reliability. In the evaluation of three underfill materials on a SBGA (Super BGA) component undergoing simulated thermal cycling, the researchers reported that underfill materials with high CTE and low modulus will increase inelastic strain at certain locations and reduce overall solder joint fatigue life. Similar results for have also been observed for CBGA components [7].

Some of the available literature concerning underfill process characterization has been sponsored by industry. Loctite Corporation has invested considerable resources in developing guidelines and specifications for process related characterization issues [10] ranging from package recommendations for underfill applications, board surface preparation and cleanliness, voiding, equipment and dispensing patterns.

Another industry sponsored paper [9] related to the underfill process attempts to evaluate fillet size through experimental design. Conclusions reached by considering

pattern, passes and volume as variables determined that fillet control is dependant on the choice of fluid and accurate control of the dispensed volume. Additional literature sponsored by this same company [12] also investigates practical requirements for underfill process automation. Topics such as optimum handling, heating, part location and dispensing are briefly mentioned.

Peer reviewed literature on process related underfill issues such as volume optimization [13] and underfill flow characterization [14] develop mathematical models for predicting underfill behavior under varying circumstances. The paper by YewChoon, et al [13], develops a model capable of estimating the operating range of the dispensing volume of a defined flip chip assembly and optimizes underfill usage. The model takes into consideration the reliability factor, e.g., presence of fillet; manufacturing tolerance of bumps size and standoff variation. The model proposed by Wen-Bin, et al [14] investigates the effect of solder bump pitch on underfill flow and estimates the flow resistance induced by the component, substrate and solder bumps providing a tool for underfill flow front prediction. Further capillary underfill characterization literature focuses on topics such as void formation models [18], curing behavior [19], or variables affecting fillet depression [20].

Although the available underfill literature is diverse and technically useful and focused, only a few papers address practical process applications for a manufacturing environment. Manufacturing guidelines for the general application and implementation of an underfill process is lacking. This project addresses the need for a method to evaluate and measure processes related to the manufacturing facets of an underfill process in the electronics industry.

3 PROPOSED METHODS AND PROJECT STRUCTURE

The analysis presented in this project covers three main areas:

Underfill Process Characterization

Best Practices for Manufacturing

Expermental Analysis

Underfill Curing Process Characterization

Experimental Analysis

Underfill Cost Analysis

Application of Yielded Cost Model

Experimental design was used extensively in the analysis of this project. Experiments were performed for the first two areas of interest and a cost model was developed for the third. For underfill development and curing oven heat transfer characterization, experiments were designed to understand the relationships existing between process variables and the responses. Underfill characterization took place on a Camalot Xyflex Pro dispensing machine while heat transfer analysis was developed on a Electrovert Bravo 8 oven. Underfill cost analysis development was based on the yielded cost metric documented in [26].

3.1 Underfill process Characterization Methodology

For underfill process characterization, a 2^4 factorial screening experiment was initially used to understand the relationship between the process variables and fillet variability. The objective is to determine what process variables and conditions minimize fillet variability around the component. Fillet variability will be calculated using the standard deviation of fillet cross sectional areas on four sides of each test DRAM (See Figure 5).
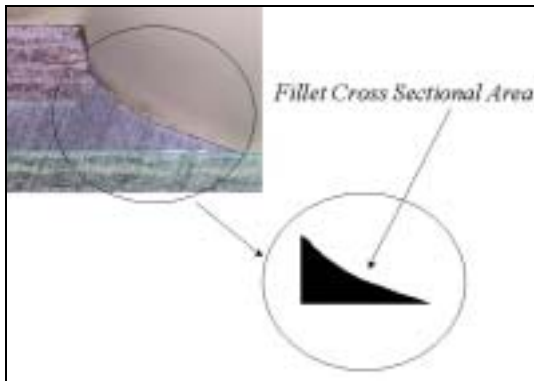
Figure 5: Example of a Fillet Cross Sectional Area

This is defined as the experiment's response variable.   Small standard deviations for fillets on a single component will indicate conditions for greater fillet consistency around the component. Large variations in fillet area around the component will indicate less favorable conditions for fillet uniformity. Fillet cross-sections will be measured using a laser-sectioning microscope (LSM).

The screening experiment will use four factors with high and low settings (a 2^4 full factorial).   These parameters are chosen based on the experience gained during preliminary tests with the underfill process. The four variables studied in this experiment are: number of passes, board temperature, needle size and dispense pattern. See Table 1 for the settings.

Table 1: 2^4 Factorial Factors for Screening Experiment

Factor	Variable
A	Passes
B	Bd. Temp.
C	Pattern
D	Needle Size

The experiment was augmented to a Central Composite Design (See Table 2) in order to obtain two response surfaces, one for each pattern.   These graphs were used to visually interpret the interactions between number of passes and board temperature for each pattern and their effect on standard deviation of the fillet's cross sectional area.

Ben Salomon

Results from the composite experiment provide information on the process characteristics, particularly in understanding optimum number of passes and temperature relationships. This information will be used for developing general process recommendations.

Table 2: Central Composite Design

Design Points	Factor	
	Passes	Bd. Temp
Extreme Min		
Lower Axial		
Center		
Upper Axial		
Extreme Upper		

3.2   Heat Transfer Characterization for underfill Application

Experiment design analysis was used for developing thermal profile evaluation criteria based on heat transfer measurements. A factorial experimental approach will be used to understand the influence of three main factors and their possible interactions on board heating rate. The development efforts will take place in two major steps. The first consisting of identifying and estimating the magnitude and direction of each factor on the response, heat transfer rate q, measured in Watts. The second stage of this experiment will consist of quantifying the test board heating effects of each factor and developing a model with the data through the use of response surface analysis. The oven for this experiment consists of eight heating zones with two cooling fans (Electrovert Bravo 8105). The experimental results will apply solely for this oven.

The original factorial screening experiment will consist of selecting three factors with high and low settings. The factors and settings listed in Table 3 were chosen based on previous empirical results and availability. The experiment will consist of a single replicate 2^3 factorial design with center points.

Table 3: 2³ Factorial Parameters and Settings

Factor	Proposed Setting
Oven Temperature	High and Low temperatures to be determined
Conveyor Speed	High and Low conveyor speeds to be determined
Convection (blower) Setting	Med High and Med Low Blower Settings (measured in cubic ft./min)

The procedure throughout the experiment will consist of recording temperature profiles on a test vehicle for each experimental condition. The test vehicle (the experimental unit) will consist of a flat plate of ECP plus material with six thermocouples attached diagonally across the plate. The average heat rate response across the experimental unit will be measured indirectly by observing the temperature increase in the six thermocouples attached to the test vehicle. Each experimental condition had a unique profile. An example profile is shown in Figure 6.
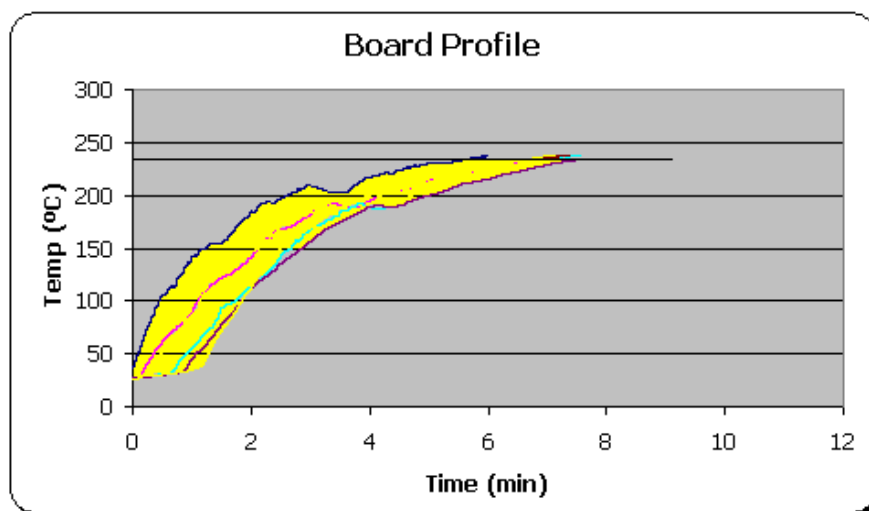
Figure 6: Sample underfill Curing Profile

In general, the procedure is to calculate the energy increase (Joules) at each thermocouple and dividing this value by the amount of time it will take to reach a predetermined point. The response, heat rate (Watts) up to this specified time, will be measured by use of the lumped capacitance method for transient conduction.

Ben Salomon

A second order model (a full quadratic) will be created using the data from the linear model above and possible additional data observations. The response surface model will be used to find optimum conditions for oven heat transfer rate and to understand the influence and interaction of each factor within an extended experimental range. The goal with this experiment is to develop a heat transfer equation as a function of conveyor speed and oven temperature.

3.3 Underfill Cost Analysis Method

Analysis of the yielded cost of processes surrounding the underfill operation was necessary in order to understand the manufacturing tradeoffs of an underfill operation. Since the underfill process is performed between two test operations, a cost model of the test/underfill/repair process was designed and analyzed based on information gathered from references [27], [28] and [29]. The yielded cost metric is documented in reference [28]. Reference [30] was used to estimate board yield after repeated rework attempts.

Yielded cost is the total cost invested per item divided by the total yield of the process under consideration [28]. The yielded cost concept as applied to this model can be interpreted as the total cost per board using the test/troubleshooting/repair (TTR underfill) process divided by the final yield. Analysis of the test process is documented thoroughly in [28].

The cost referred here is the total cost per board accrued during the various operations. The final yield is determined by the yield of individual operations, scrap generation, the effectiveness of the test coverage and the possibility of false positives created by the test operation.

The basic formula used for the yielded cost metric is,

$$C_{yielded} = \frac{C_{out}}{Y_{out}}$$

This metric quantifies Test Troubleshooting Repair and underfill (TTR underfill) strategy based on cost and quality. Determining yielded cost will be the model's objective and will be used to compare different underfill and rework scenarios. The general approach presented here is to calculate and compare the yielded cost for a fixed number of rework attempts given a defined set of inputs. A spreadsheet (testmodel.xls) was developed to aid with the model's iterations and equations. Graphical tools were used to understand the cost impact of an underfill operation on the overall yielded cost metric.

4 RESULTS

4.1 Manufacturing Best Practices

Reliable underfill processes and high yields depend on correct manufacturing methods. The following sections describe practical guidelines for implementing an underfill process.

4.1.1 Basic Design Recommendations for underfill Applications

Overall underfill flow performance and integrity can be influenced by the following array design characteristics:

Table 4: General Design Guidelines for BGA's Requiring underfill

Feature	Recommended
Ball Array layout	Array should be evenly distributed under component. Keep pitch > 0.55mm
Wetting Surface Area	Minimize soldermask breaks. Provide the best possible soldermask registration.
Solderball height	Keep gap between component and board between 0.2 and 0.3 mm
Package Size	Keep package area between 8 and 17 mm^2.
Board Thickness	Keep board thickness greater than 1.25 mm.
Keepout	Plan 85 mils keepout from components that will be underfilled.
Rework	No rework possible on underfilled components with capillary underfill.
Vias	Vias under the component must be filled, and covered with soldermask
Pad area	Minimize pad and non-soldermasked areas.

Ben Salomon

Components and boards must be free of flux residues, contamination, or non-intended soldermask discontinuities where underfill will be applied. These will cause a slower moving wave front eventually leaving voids within the underfill material.

4.1.2   Storing and Handling of underfill Materials

All underfills must be supplied with (Material and Safety Data Sheet) MSDS documentation. Capillary underfills are usually stored at –40º C. Storage at higher temperatures may significantly shorten shelf life. Lower temperatures than –40º C provide a small extension of shelf life with the possibility of increasing the incidence of entrapped air within the cartridge during thaw. Uncured underfill changes over time regardless of storage conditions. Use of expired underfill material is not allowed.

Underfill material is shipped in insulated containers that maintain it at sufficiently low temperatures far beyond the transit time. Underfill material received at temperatures higher than –40º C must not be used. Underfill material is packed with dry ice around an inner box containing the underfill material. This inner box should not be opened at room temperature and should be place into a designated freezer for a minimum of eight hours before use. This allows the underfill to warm slowly from dry ice temperature to –40ºC. It is highly recommended to inspect and store an underfill shipment as soon as it arrives and it is not recommended to leave newly arrived unopened underfill shipments in the receiving area for more than 8 hours. Store the inner box containing underfill material immediately after the shipment container is opened and inspected. Storage above recommended temperatures significantly shortens the shelf life of underfill.

When ready to use, underfill cartridges must be thawed at room temperature between one and two hours with their tips down. Abrupt changes in temperature during thawing may result in air pockets or voids in the underfill material. Constituents of liquid underfills do not truly "freeze" even at –40ºC. The chemical crosslinking reactions advance at a very slow rate during cold storage in a process called "advancement". Expired cartridges should be discarded since underfill material is compromised by

advancement during extended storage. Refreezing unused or leftover used underfill material is not allowed under any circumstances.

Depending on application requirements, underfill packaging may come in a variety of different size syringes or cartridges. Smaller 10cc cartridges are used for low volume applications while higher volumes may use 40cc or larger 6 oz. cartridges. Advancement accelerates after thawing and proceeds even more quickly at the temperatures found within the dispensing equipment. Eventually the viscosity will exceed that which provides acceptable processing, rendering the underfill useless. The period during which the underfill is processable is called the pot life. underfill whose 8-hour pot life is exceeded must be discarded. For this application typical pot life is limited to one shift or 8 hours. Ideally, inspection and storage should be made as soon as shipment is received.

Underfill Material Storage and Handling: General Summary

- ❑ Receive underfill material. Unopened shipment must not stay in the Receiving area for more than 8 hours.
- ❑ Inspect Shipment Temperature. Do not open inner box containing underfill material.
- ❑ Place inner box containing underfill material in a –40ºC freezer for at least 8 hours before using. Do not handle underfill material without first reading the MSDS. Personal protective equipment, hazards, physical properties, first aid and fire fighting measures, spill cleanup and other issues are discussed in the MSDS document. Since underfill chemistry can vary greatly, read the MSDS of each underfill to be handled.
- ❑ Thaw required quantity of cartridges for at least one hour when ready to use.
- ❑ Once thawed, pot life is limited to 8 hours. underfill exceeding this limit must be discarded.

4.1.3 Underfill Dispensing

This section describes process related conditions for underfill dispensing.

The main underfill process objective for this application is to consistently fill the gap between the board and the specified component in an efficient and reliable manner with the best possible underfill material. Other process objectives include:

- ❑ Minimizing voids-under the component.
- ❑ Finding the best dispensing pattern.
- ❑ Avoiding underfill material contact with other components.
- ❑ Optimizing process cycle time and process flow.

The following guidelines are based on underfill development investigations using the following materials and equipment:

- ❑ Dispenser: Camalot Xyflex Pro
- ❑ Freezer: Scientemp Model 51-12
- ❑ Curing Oven: BTU Paragon 150
- ❑ PCB Supplier: Hitachi and Honeywell
- ❑ MAKO PCB soldermask: Hitachi Probimer 77 Honeywell Enthone-Enplate DSR 3241G (CR) -
- ❑ Pegasus Component soldermask: Taiyo PSR 4000
- ❑ Underfill: Loctite/Hysol 4531

Changes in materials (component or PCB soldermask or underfill material) may require prequalification and review by interconnect reliability engineering.

The effect of voids on component reliability was researched by interconnect reliability engineering. A degree of void formation is inevitable and acceptable within certain limits. See Section 6 for acceptability regarding voids. Voids are caused by the inclusion of air, other gases, solvents or moisture beneath the component, around solder balls or at soldermask discontinuities. Poorly wetted regions in the underfill's path may cause voids, as will opposite fluid fronts during the underfill flow. The wrong timing of

Ben Salomon

dispensed passes may also cause air entrapment. Refer to Figure 7 for an example of a void formed at a soldermask discontinuity.
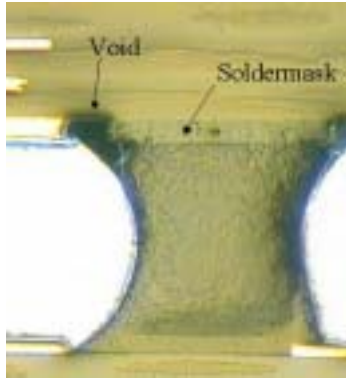
Figure 7: Example of an Underfill Void at Soldermask Discontinuity

Although board cleanliness prior to underfill is critical for component reliability, washing the board prior to underfill is not cost effective or required for this application. Experiments during development have shown that an exclusive cleaning process prior to the underfill operation does not significantly improve reliability for this application.

Control of underfill deposition depends on the following:

- ❏ Needle Type
- ❏ Pump Flow Rate
- ❏ Dispense Volume
- ❏ Board Temperature
- ❏ Dispense pattern
- ❏ General Process parameters/Tooling

4.1.3.1 Needle Type

Needle diameter controls the line width during dispensing. Experiments indicate that gauge 21 or 22 needles are appropriate for this application.   Needle heating is not required. Needle characteristics are shown in Table 5.

Table 5: Needle Chart

Gauge	Internal Dia		External Dia	
	in	mm	in	mm
20	0.024	0.61	0.036	0.91
21	0.020	0.51	0.032	0.81
22	0.016	0.41	0.028	0.71
23	0.013	0.33	0.025	0.64
25	0.010	0.25	0.020	0.51
27	0.008	0.20	0.016	0.41

4.1.3.2 Pump Flow Rate Control

Controlling the flow of dispensed material is important since component reliability is influenced by the amount of deposited underfill.   Underfill flow rate is machine controlled by regular automatic measurement of underfill mass per unit time. Automated calibration of dispensed mass insures that each pass has the correct amount of fluid regardless of changes in underfill viscosity over time, needle size or underfill volume in the syringe.   The linear positive displacement piston pump (Figure 8) used for this application is typically within 5% of target mass and is regarded within the industry as the best type of pump available for underfill dispensing.

Figure 8: Linear Displacement Piston Pump

4.1.3.3 Volumetric Requirements

Volumetric and mass measurements made during underfill development of the sample DRAM components indicate that complete underfill coverage of the BGA component with well-formed fillets extending beyond the edges was possible with 0.205 ± 0.015 g. The volume equation in Table 6 presents the approach used to predict the amount of material required for dispensing underfill for this specific component. For the equation in Table 6, the fillet volume estimate requires a "shape factor" parameter that is dependent on the type of underfill and its wetting properties. If shape factor information is lacking, a reasonable fillet a priori volume approximation may be obtained by assuming small triangular fillets around the perimeter of the component. In reality the solder balls are not spherical. The formula given for V_b however is sufficient for an initial approximation.

Figure 9 presents the relationship between underfill contact angle and shape factor for this specific application using Loctite/Hysol FP4531 underfill at 90ºC. Contact angle will vary depending on temperature, viscosity, surface conditions, and volume constraints.

Fillet contact angle provides a general indication of the wetting characteristics for a particular fillet and is one of the criteria used to determine fillet integrity.

Table 6: Underfill Volume Approximation

$V_u = V_c - V_b + V_f$

Where V_u = Total underfill volume

V_c = Volume under the component = (Component length) x (Component width) x (underfill Gap)

V_b = Volume approximation of the solder balls* =
[(4π/3) x (ball radius)^3] x (number of joints)*

V_f = Fillet Volume = [(Fillet Height) x (Fillet Width) x (2) x (Component Perimeter) + [(Fillet width) 2 x (Fillet height) x (π/3)] x (Shape Factor)
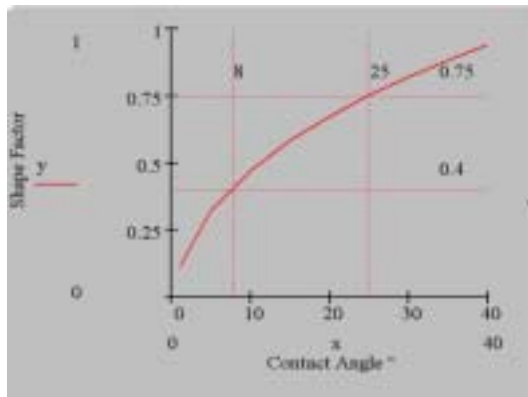
Figure 9 Shape Factor vs. Contact Angle Process Window

Figure 10 illustrates the contact angle concept on a sample fillet cross section. Development for this application has demonstrated that the process is sufficiently

robust to allow for simple visual discrimination analogous to that used with solder joints during inspection by operators.
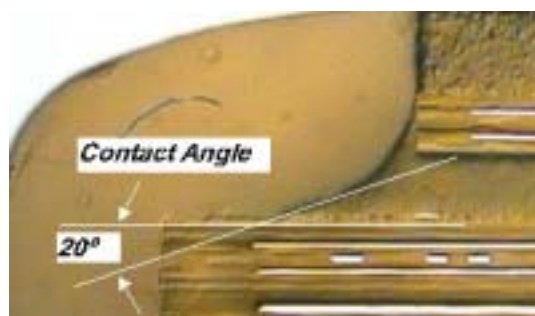
Figure 10: Contact Angle Measurement

Experiments with Hysol FP4531 self-filleting underfill have determined that the shape factor for this particular application is in the range of 0.4 and 0.75 for a contact angle of 8 and 25º respectively.

4.1.3.4 Board Temperature

The recommended board temperature for this application according to the underfill supplier is 90ºC. This temperature provides for fast flow rates and excellent wetting characteristics while delaying the onset of gelling for a sufficient amount of time. Boards for this application require hot air convection heating, provided by the underfill dispensing equipment, immediately prior, during and after the underfill operation.   Typical hot air temperatures at these stations will range from 100ºC to 120ºC. Ramping to the dispensing temperature requires approximately 7 minutes.

4.1.3.5 Dispense Pattern

The recommended dispense pattern for this application is the "L" shaped pattern (See Figure 11). This pattern optimizes process cycle time without compromising product quality and was found to provide the most uniform fillet around the BGA. The Results Section discusses the experimental results that demonstrate the

advantages of this pattern over a straight line-dispensing pattern. This specific application requires two "L" pattern passes to dispense the required volume of material.
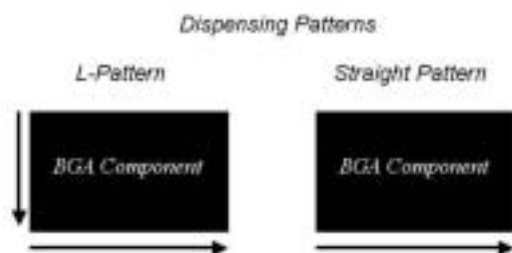
Figure 11 L Shaped and Straight line underfill Dispense Patterns

The first pass provides a reservoir of underfill for initial wetting of the board and component surfaces and the second pass dispenses the remaining amount of material for complete underfill coverage. This second pass will generally determine the final fillet size. A final "filleting pass" is not required since Loctite FP4531 is a self-filleting underfill.

From a process perspective, a higher number of passes may increase cycle time due to idle waiting between passes while the fluid wavefront propagates under the component (flow-out). Too few passes will sacrifice flow and fillet-width control.

The use of a process carrier in this specific application allows processing of 12 boards (a batch) per recipe. This flexibility reduces conveyor-handling time and allows dispensing patterns to be staggered. This staggering significantly improves cycle time by allowing a dispense operation during an otherwise idle flow-out. See Figures 12 and 13. Underfill recipes must be designed to optimize flow and dispensing times. Typical processing time at the dispensing station for this particular application have been measured to take between less than ten minutes. The recommended number of passes for this application is two.

First Pass Dispensing, First Group (Approx time: 2 min)
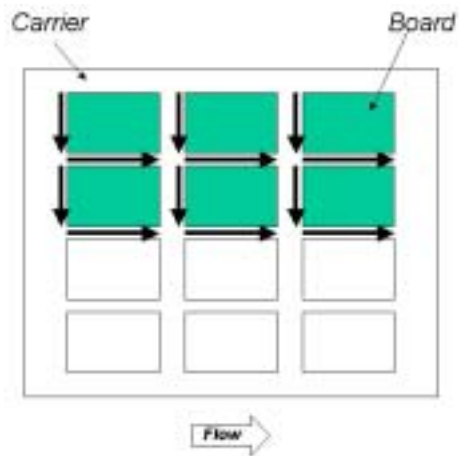
Second Pass Dispensing, First Group (Approx. time: 2 min)
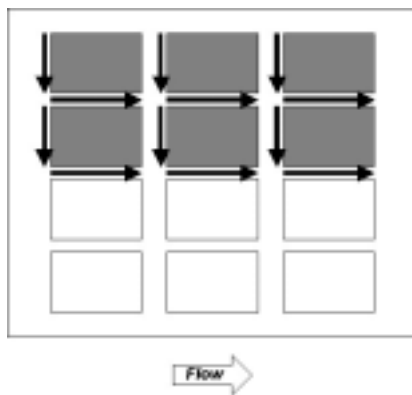
First Pass Dispensing, Second Group (Approx time: 2 min)
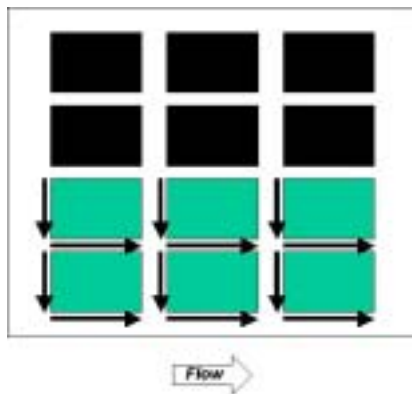
Figure 12 Recommended Batch Dispensing Sequence

Ben Salomon

Second Pass Dispensing, Second Group (Approx time: 2 min)
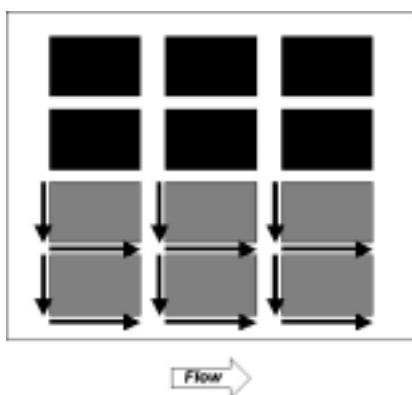
Complete Flowout (Approx time: 2 min at Postheat)
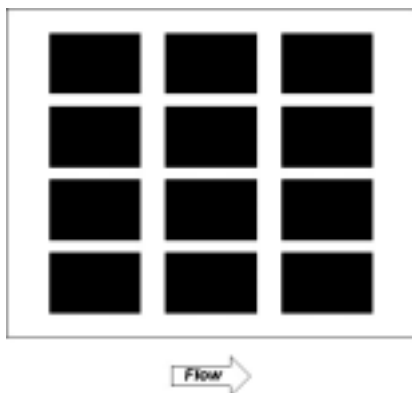
Figure 13 Recommended Batch Dispensing Sequence (Continued)

Air entrapment is minimized by programming the correct timing between the first and second passes. For two passes it was found that no more than 60 seconds between passes provides sufficient time to avoid air entrapment. Dispensing the entire required underfill in one pass was impossible without flooding and contaminating adjacent areas. Programming more than two passes allowed for marginal process improvements but increased cycle time by 15%.

Ben Salomon

4.1.3.6 Other Process Parameters and Tooling

Other dispensing parameters such as needle position and height are easily controlled and are programmable on the underfill machine. Dispensing close to the component as possible gives tighter control over the final fillet geometry and provides for quick capillary action as soon as the underfill material contacts the ball array area. For this application this distance is 250μm (approx. 10 mils). Needle geometry for most commercial underfill applications is straight. Special applications may require special modifications such as needle heating to aid the dispensing process.

Consistent dispensing height provides uniformity and helps controls stringing (the tendency of a bead of underfill to remain at the tip of the needle after a dispense pass). Dispense height during development was set at 250 μm and was found to provide sufficient clearance for the needle over the board surface. A programmable backward and upward movement into the dispensed underfill material was used to control stringing after each pass.
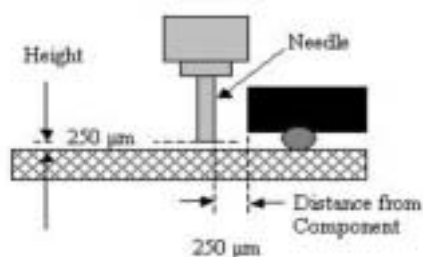
Figure 14: Typical Needle Placement for underfill process (not to scale)

The actual distance from the component is related to machine x/y accuracy and the tolerances within the process carrier holding the board in place. No significant variations in needle placement were noticed during development either with machine accuracy or process carrier tolerances.

Ben Salomon

Observations made during development indicate that flow time will increase the further the needle distance is from the component during dispensing (see Figure 14). Beyond this distance, underfill material will leave more residue and a wider fillet at the dispensing edge.

Varying dispensing height from the recommended for this application increased the likelihood of unwanted underfill material on component surfaces or damaging the needle.

A typical underfill process carrier is the only external tooling required for this process. Figure 15 illustrates a board in one of the pockets of the process carrier. No tooling pins or hold-downs are necessary for this operation.

Printed Circuit Board
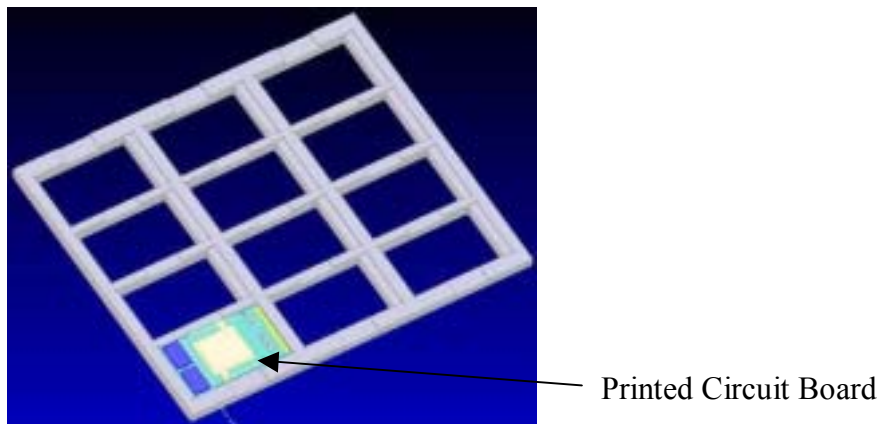
Figure 15: Typical Underfill Process Carrier

4.2   Underfill Application Process Characterization

Process development efforts focused on identifying critical underfill parameters for this specific process and determining a range of operability.

4.2.1   Screening Experiment

A 2^4 factorial screening experiment was initially used to understand the relationship between the process variables and fillet variability. The objective was to determine what process variables and conditions minimize fillet variability around the component. Fillet variability was calculated by using the standard deviation of fillet cross sectional areas on four sides of each test DRAM (See Figure 16). This was the experiment's response variable.   Small standard deviations for fillets on a single component would indicate conditions for greater fillet consistency around the DRAM.   Large variations in fillet area around the component would indicate less favorable conditions for fillet uniformity. Fillet cross-sections were measured using a laser-sectioning microscope (LSM).
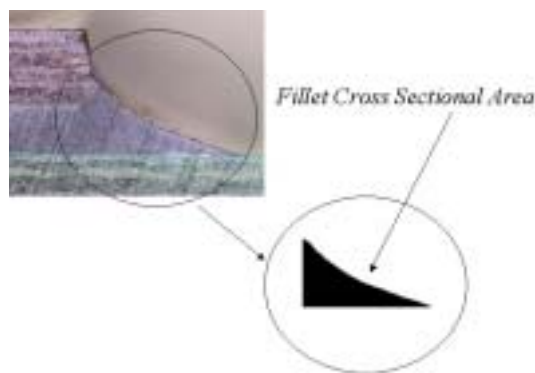
Figure 16: Fillet Cross-Section for one side of a test Dram

The screening experiment used four factors with high and low settings (a 2^4 full factorial).   These parameters were chosen based on the experience gained during

preliminary tests with the underfill process. The four variables studied in this experiment were: number of passes, board temperature, needle size and dispense pattern. See Table 7 for the settings.

Table 7: Factorial Settings

Factor	Parameter	Setting
A	Passes	Low (4) High (8)
B	Bd. Temp.	Low (65) High (90)
C	Pattern	L and Straight pattern
D	Needle Size	Low (25 gage) High (20 gage)

The initial screening experiment demonstrates that needle size did not significantly affect overall results. Most significant factors affecting fillet variability around the DRAM were the number of passes and the type of dispense pattern. Figure 17 compares the magnitude of each effect against a statistical level of reference (α = 0.05) after disregarding needle size as a factor.
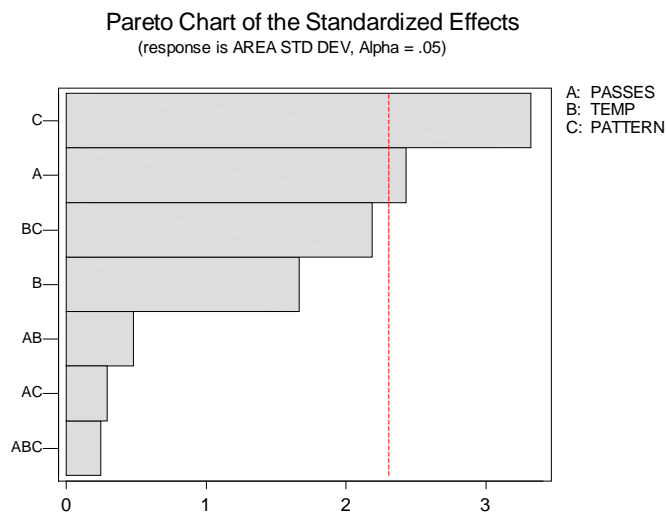
Figure 17: Screening Experiment Comparison of Effects

4.2.2   Central Composite

The experiment was augmented to a Central Composite Design (See Table 8) in order to obtain two response surfaces, one for each pattern.   These graphs (Figures 18 and 19) were used to visually interpret the interactions between number of passes and board temperature for each pattern and their effect on standard deviation of the fillet's cross sectional area.

Table 8: Central Composite Design Settings

Design Points	Factor	
	Passes	**Bd Temp**
Extreme Min	2	58
Lower Axial	4	64
Center	6	77
Upper Axial	8	90
Extreme Upper	10	95

Ben Salomon

STRAIGHT PATTERN RESPONSE SURFACE FOR FILLET STD. DEVIATION
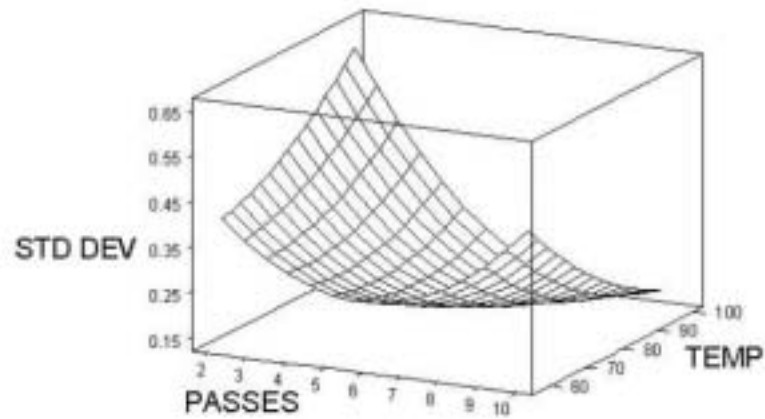
Figure 18: Fillet Cross Sectional Variability Surface Plot Straight Pattern Dispensing

L PATTERN RESPONSE SURFACE FOR FILLET STD. DEVIATION
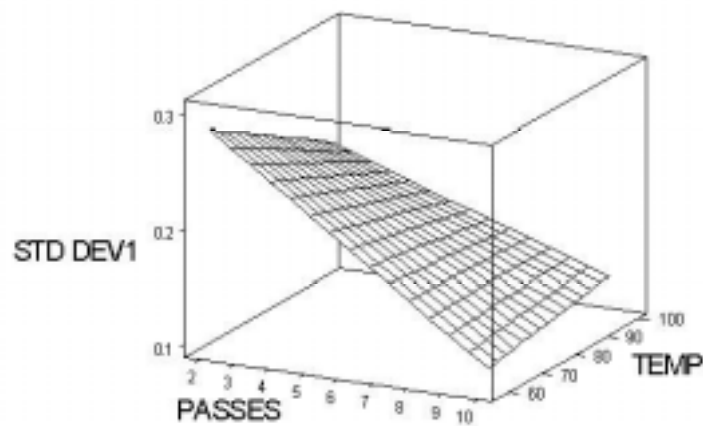
Figure 19: Fillet Cross Sectional Area Variability Surface Plot for L-Pattern Dispensing

Ben Salomon

The general interpretation from these graphs indicates that dispensing at higher temperatures and with increased number of passes will reduce fillet variability around the test component. Dispensing in an L pattern seems to offer greater predictability over a wide range of operability with respect to the alternative straight pattern. . The contour plots (see Figure 20) for these two surfaces indicate that the L pattern is better suited to operate with higher temperatures (e.g. 90ºC) and fewer passes when compared with the straight dispensing pattern.

From a process perspective, *higher dispensing temperatures* and *fewer passes* provide greater efficiencies. Figure 20 indicates that the L-pattern yields greater predictability with regards to fillet uniformity than straight pattern dispensing under the same operating conditions and produces overall less fillet variability, especially in the region of interest (e.g. high temperatures and 2 or less passes).

4.2.3   Process Window

This section details operating conditions for this underfill application on Camalot Xyflex Pro equipment. The above characterization was used as the basis for developing the required underfill recipe for this product. The countour plots in Figure 20 illustrate available process windows for two dispensing alternatives. The process with less fillet variability was chosen (the L-pattern) at a setting with a minimum number of passes (2 passes) at a temperature that allows quick underfill flow-out time (90-95ºC). The required information to develop an underfill recipe for the Xyflex-Pro underfill dispensing machine is presented in Table 9.

4.2.4   Cure Profile

This section reviews the recommended curing profile and discusses the effect of moisture on underfill quality**.** Recommended cure schedule for Loctite FP4531 is 7 minutes dwell at 160ºC. Heating rates of greater than 10ºC/minute are recommended

to reduce loss of chemical agents prior to cure. A specific cooling rate is not required for this underfill
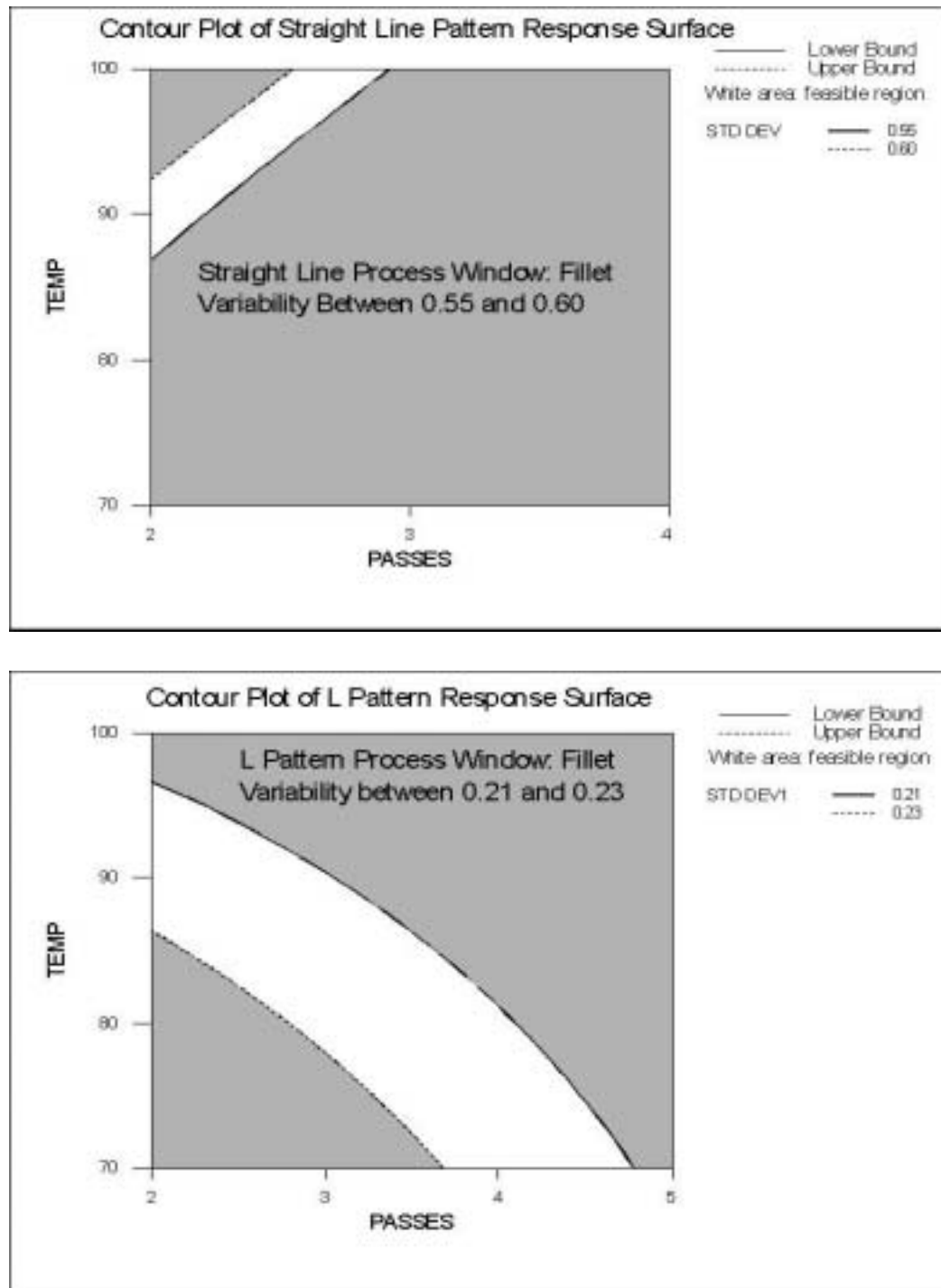
Figure 20: Line Pattern Dispensing Process Windows

Table 9: Parameters for underfill Typical Recipe

Parameter	Settings Range	
	Low	**High**
Line Width (mm)	300	400
Line Lift Height (mm)	n/a	0.025
Move Lift Height (mm)	n/a	0.6
Dispense Height (mm)	n/a	0.025
RPM	360	400
Timeout (sec)	30	60
Fiducial Threshold	75	90
Preheat Duration (sec)	480	600
Post Heat Duration (sec)	420	480
Preheat Station Temp (°C)	110 °C	125° C
Dispense Station Temp (°C)	90°	100°
PostHeat Station Temp (°C)	90°	100°
Syringe Temp. (°C)	35°	40°
Air Pressure (psi)	15	30
Cure temperature	160 °C	170° C

material. Figure 21 presents the profile developed for this underfill using a 10 zone BTU reflow oven. Table 10 lists the temperatures for each zone. Belt speed for the required dwell time is 11.0 inches/minute. Total processing cure time using this oven

was measured at 18 minutes. See section 4.3 for a full underfill qualification of the curing oven equipment.

4.2.5   Exposure to Moisture

Loctite recommends that exposure of uncured underfill to the ambient atmosphere be limited to one hour. Underfill that is contaminated by moisture prior to cure often exhibits a whitish appearance after cure. The cured underfill may exhibit very poor

Table 10: Curing Profile Oven Temperatures

ZONE	TEMPERATURE (ºC)	
	Bottom	Top
1	190	190
2	200	200
3	180	180
4	175	175
5	170	170
6	170	170
7	170	170
8	170	170
9	170	170
10	170	170
Cooling	30	30

	Peak	Total Time Above 160	Total Time Above 170	Pointer 0.3	Slope 0.32	Pointer 0.6	Slope 7.13	Pointer 7.9	Slope 59.29	Pointer 66.1	Slope 47.36	Pointer 113.4	Slope 14.26	Pointer 127.7
1 CCGA	170.6	677.91	19.35	23.7	0.00	23.7	0.01	24.2	0.44	164.9	-0.00	164.1	0.02	165.5
2 DRAM	169.9	674.40	0.00	23.7	0.00	23.7	0.02	24.5	0.45	165.3	-0.02	160.7	0.06	165.5
3 DRAM	169.6	657.20	0.00	24.0	0.00	24.0	0.00	24.0	0.45	165.7	-0.02	160.5	0.07	166.0
TC Meas	170.0	673.20	6.45	23.8	0.00	23.8	0.01	24.2	0.44	165.6	-0.02	161.7	0.05	165.6

Figure 21:Profile Developed for Underfill Cure Loctite FP4531

solvent resistance or depressed thermal stability and lower glass transition temperatures. These effects are most visible in the fillet region. This application specifies post heat durations of between 7 and 8 minutes prior to entering the curing oven. See Table 9.

4.2.6 Process Flow

This section presents process flow requirements. The flowchart in Figure 22 summarizes the necessary steps required for this double-sided underfill process. As mentioned previously board cleaning is not required for this application. Two operators will be monitoring the process: one at the underfill machine and another for inspection and handling.

The preheating stage removes moisture and heats the board to its optimum temperature. Heat is continuously applied throughout preheat, dispensing and post-dispense operations. Post heat after dispensing is required in order to have the underfill maintain the required flow and form fillets within the allotted time frame.

Processing time from beginning to end for a batch of 12 double-sided boards was estimated at 60 minutes.

Normal processing time at the post-heat stage is between 7 and 8 minutes. Preheat board temperature is 90ºC and inspection is visual based on fillet integrity and geometry. The pot life published for FP4531 is 8 hours. Table 11 summarizes this information.

Table 11: Process Times for MAKO Batch processing

Stage	Appox. Batch Times
Pre-heat	7~9 minutes
Dispense	8~10 minutes
Post-Heat	7~8 minutes
Oven	18 min
Inspection	1 min
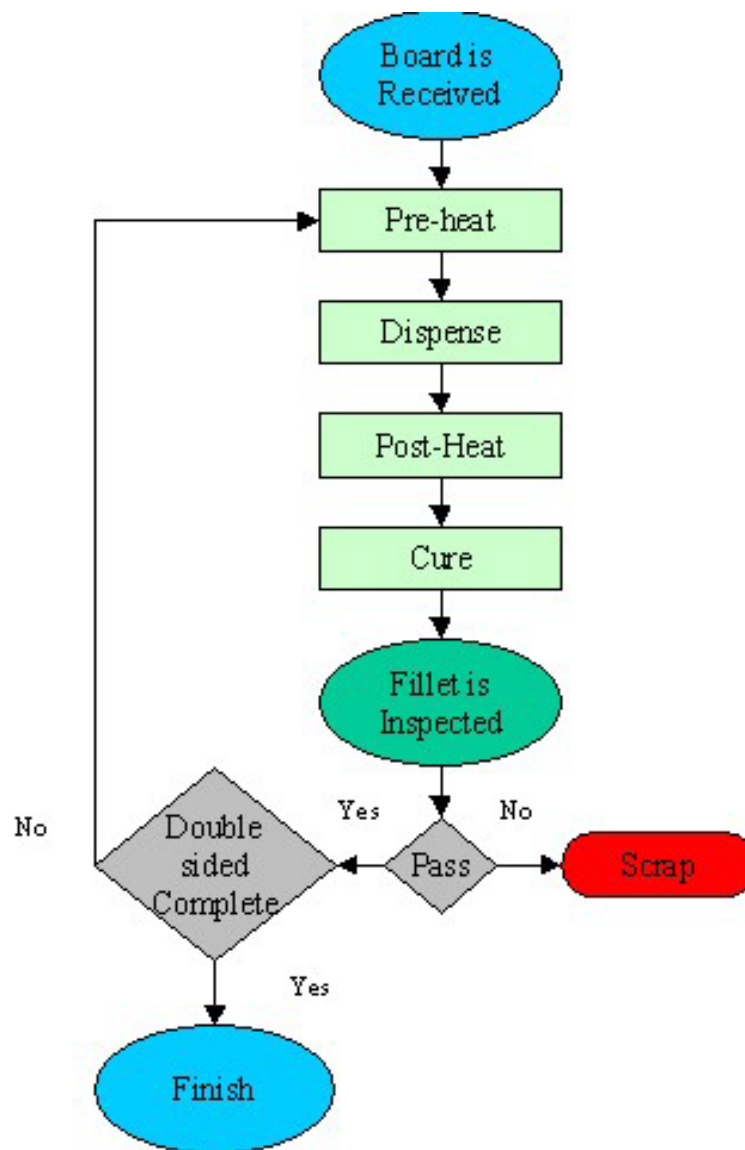
Figure 22: Simplified Process flow for an underfill process

4.2.7 Troubleshooting

This section (Tables 12 through 14) presents a troubleshooting guide for the process engineer and a fishbone analysis (Figure 23) of the underfill process.

Ben Salomon

Table 12: Underfill Process Troubleshooting Table

Problem	Possible Cause	Solution
Voids in Syringe	Improper thawing procedure	Follow recommended thaw procedure
Voids in underfill located next to solder ball joints.	Moisture in board or package	Dry (bake) board before underfilling
	Poor wetting at solder ball	Improve soldermask registration/Avoid unnecessary soldermask openings. Use soldermask defined pads Raise temperature at dispense station
Voids in underfill randomly located under die.	Flux residues	Raise board temperature. Maximum board temperature for this underfill is 100ºC. Check solder paste flux % or type of flux
Voids in underfill always at the same location away from dispense site	Dispense lines are too long.	Reduce length of dispense line. Change pattern.
Voids in underfill always at the same location close to dispense site	Air pulled under component at dispense location due to depleted dispense fillet	Reduce time between successive passes.

Table 13: Underfill Process Troubleshooting Table(Continued)

Problem	Possible Cause	Solution
Voids in fillet	Moisture or volatiles escaping from board or component	See above section for moisture
Dripping from needle	Underfill too fluid	Syringe temperature too high
	Air in dispense line	Purge air from dispense line
	Excess back pressure in needle of positive displacement pump	Reduce dispense speed
	Pump control	Reduce syringe pressure "Back-track" needle after each dispense line. Change needle
Stringing of underfill during dispensing	Needle too high	Lower needle to 10mils above board
	Needle withdrawn too quickly	Delay upward motion after dispense operation
	Pot life exceeded	Change underfill cartridge
	Expired shelf life	Same as above
Underfill flows extremely slow under component	High viscosity	Raise board temperature. Maximum board temperature for this underfill is 100ºC.
	Pot life exceeded	Change underfill cartridge
	Gap is too narrow for underfill	Change underfill or gap height

Ben Salomon

Table 14: Underfill Process Troubleshooting Table(Continued)

Problem	Possible Cause	Solution
Dispensing is difficult or inconsistent	Underfill not thawed	Follow thaw procedure
	Pot life exceeded	Change underfill cartridge
	Pump back pressure too high	Change needle
Underfill will not cure	Insufficient cure time	Check dwell time
	Oven temperature too low	Check oven profile
	Contaminated underfill cartridge	Change underfill cartridge Check underfill exposure time to ambient temperature
Abnormal surface appearance after cure	Moisture contamination	Same as above
Underfill does not form fillet	Insufficient volume	Dispense more underfill
	Poor wetting on board surface	Raise board temperature Remove silkscreen ink, ground traces or EMI shielding lines in underfill flow path.

Figure 23 presents an Ishikawa diagram (fishbone) that summarizes some of the information discussed so far.

Underfill Yield Fishbone

Figure 23: Process Fishbone Representation

4.2.8   Acceptability Criteria

This section presents criteria that may be used to develop an inspection aid for the underfill process.   Although inspection for voids beneath the component is not necessary in a production environment, the following photos illustrate what was observed during development. Tests performed at Fort Collins have demonstrated that: for Dexter [Loctite FP4531] underfill the only sample of parts that failed to meet reliability requirements were reworked parts that also had [experimental] voids and no underfill fillets. Development of an underfill workmanship specification focused on: deliberately-induced interior voids, missing fillets, and DRAM rework (replacement) prior to underfill.

The following photographs (Figures 24 through 29) show representative failures caused by the above-induced defects. In general interior-causing voids had a more severe impact on fatigue life than undersized fillets.

UNACCEPTABLE

Any voids visible in underfill fillets
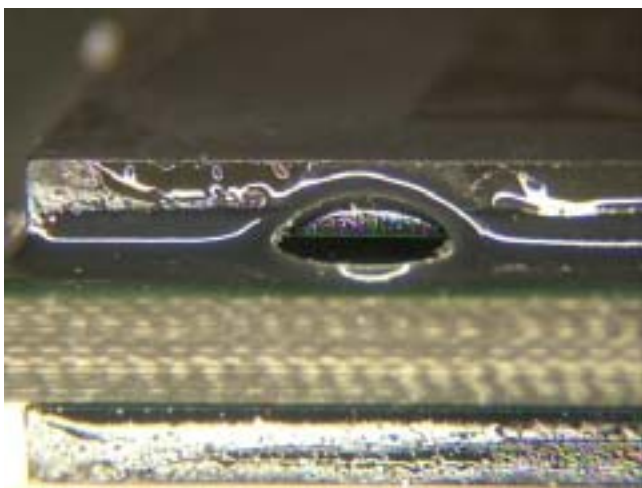
Large void in Underfill Fillet. Fillet size and shape is otherwise acceptable.

Figure 24: Acceptability Photos

Ben Salomon
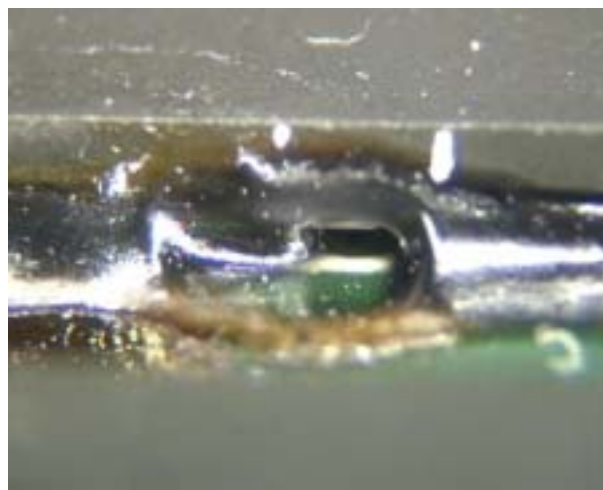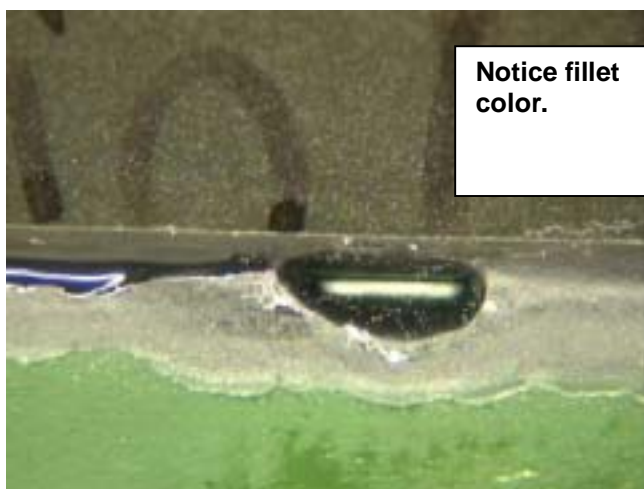
UNACCEPTABLE

UNACCEPTABLE

Fillet does not reach lower corner of component
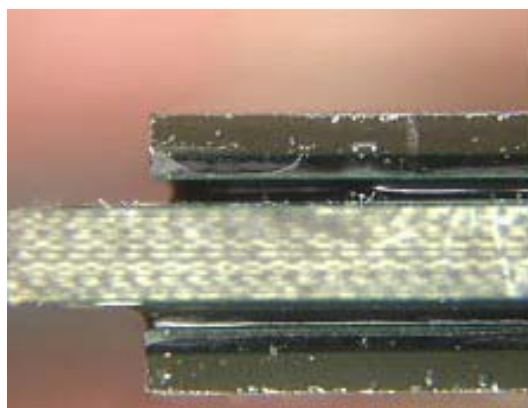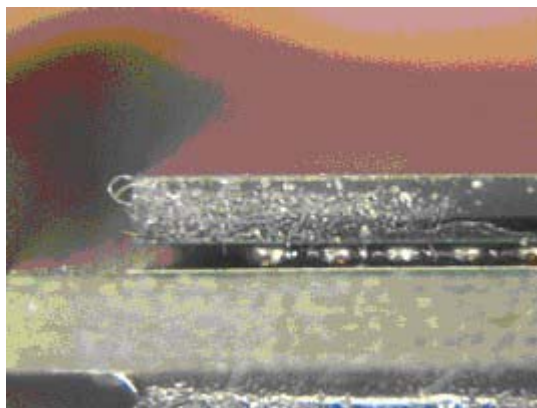
Figure 25: Acceptability Photos (Continued)

Ben Salomon

ACCEPTABLE

Fillet extends to corner of the DRAM and up the side of the component some distance.

Unacceptable fillet size (upper component),

Preferred fillet shape
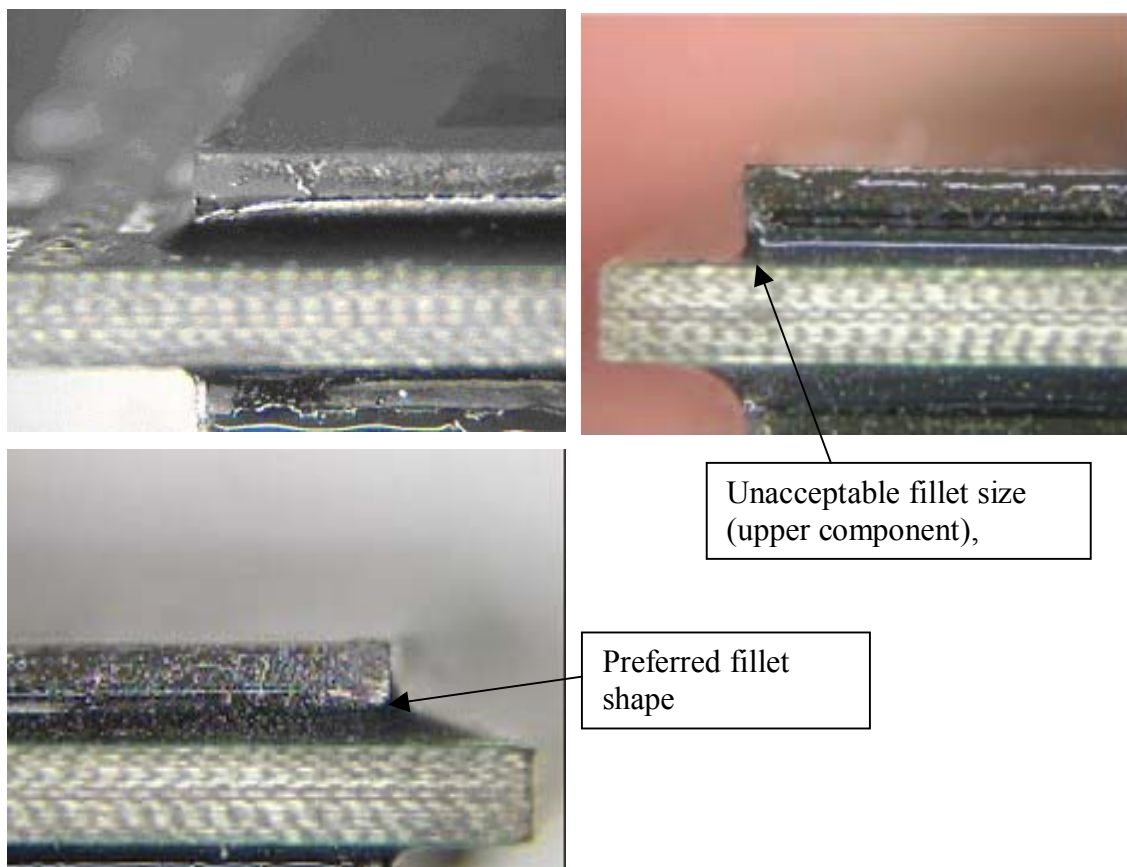
Figure 26: Acceptability Photos (Continued)

ACCEPTABLE

Voids in underfill near top or bottom corners of solder balls. Cross sectional inspections were only required during development. This type of inspection will normally not be required in a production scenario.

ACCEPTABLE VOIDS
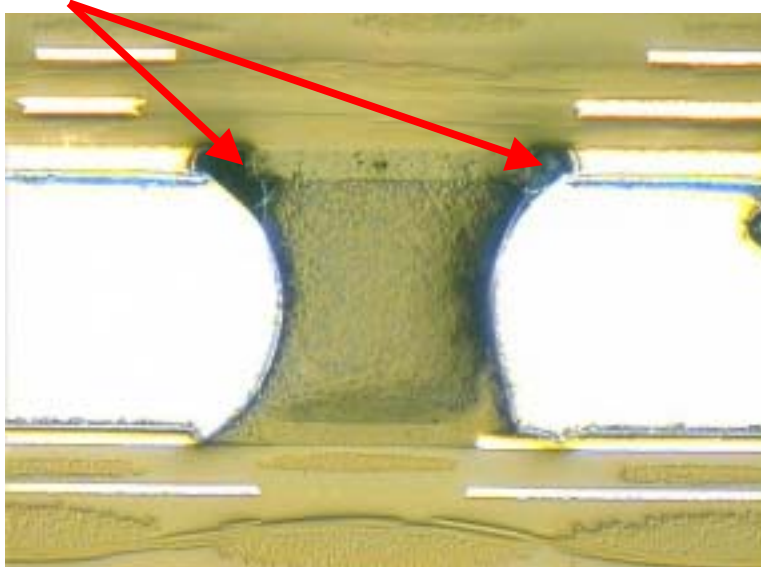
UNACCEPTABLE

SHAPE FACTOR

Contact angle exceeds 25º
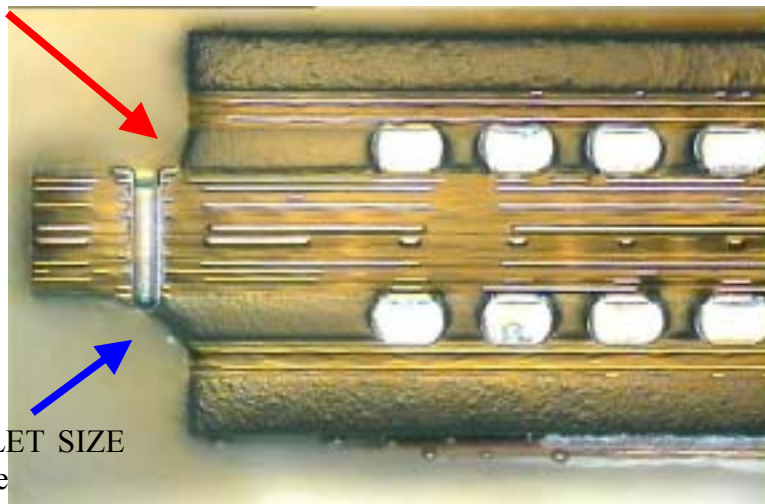
MINIMUM FILLET SIZE
70º Contact Angle

Figure 27: Acceptability Photos (Continued)

Underfill fillet reaches to bottom of package substrate. Notice poor location of via.

ACCEPTABLE Underfill fillet reaches up about 1/3 of package height (to top of package substrate) – seen on parts passing 5k cycles.

Minimum fillet size–
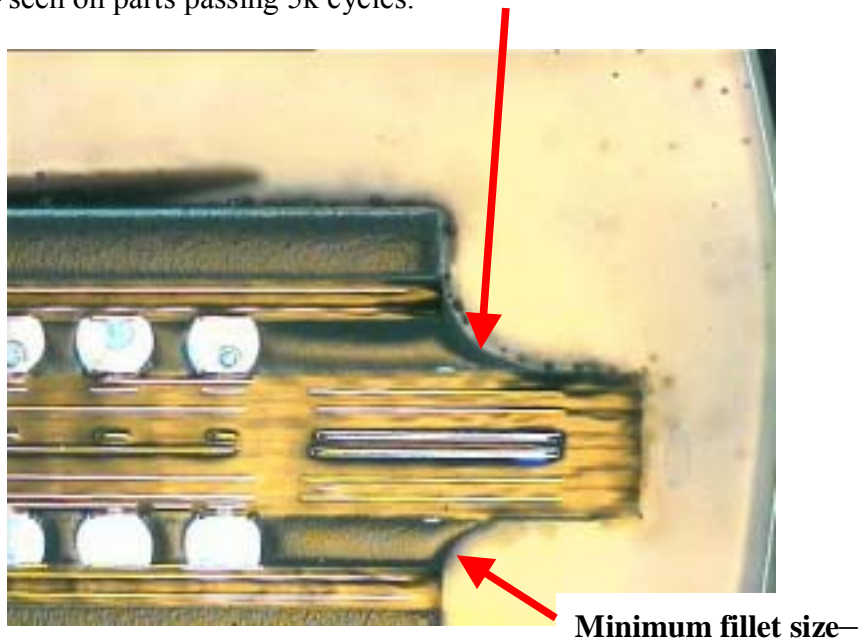
ACCEPTABLE Assuming dark area at the edge of the solder balls does NOT represent a void in the underfill beyond the area noted with a small red circle in this photo.

Void in underfill
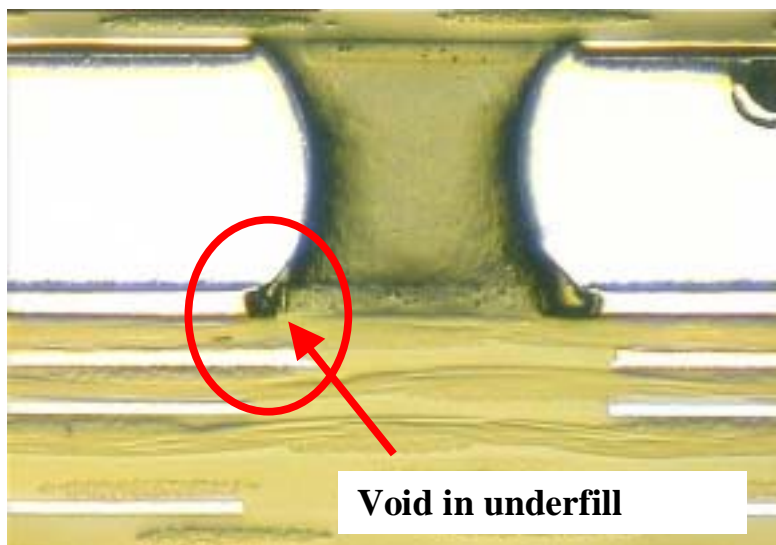
Figure 28: Acceptability Photos (Continued)

Recommended and Minimum Acceptable
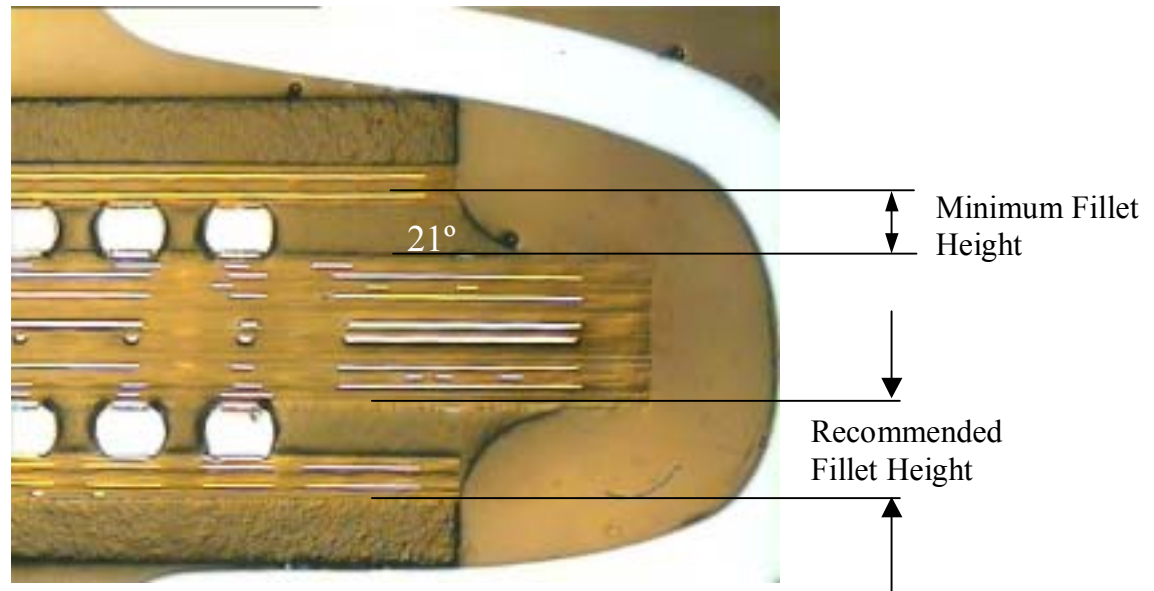
Figure 29: Acceptability Photos (Continued)

Accept marginal fillets if:

Height requirement is met, shape factor criteria is met (contact angle between 8º and 25º as shown in Figure 30), and no voids or surface irregularities are present on the fillet around the perimeter of the component.
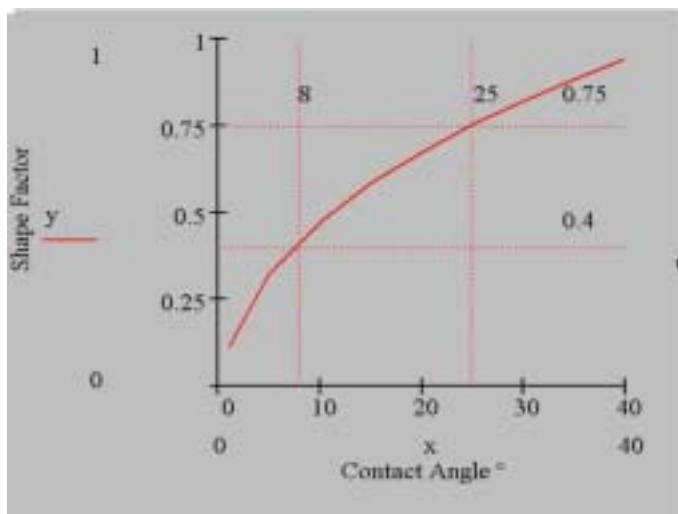
Figure 30: Fillet Shape Factor vs. Contact Angle

Ben Salomon

Inspection is 100 percent visual using the same recommended visual inspection tools used for solder joint inspection. If contact angle estimation is required use go and no-go samples for reference and comparison.

4.3   Underfill Curing Process Characterization

The following is a summary of development efforts completed on the Electrovert Bravo 8105 reflow oven. The main objective of this effort is to characterize the equipment for its general intended use and quantify the influence of chosen process variables on the heat transfer rate of a specific experimental unit.

A factorial experimental approach was used to understand the influence of three main factors and their possible interactions on board heating rate. The development efforts took place in two major steps. The first consisting of identifying and estimating the magnitude and direction of each factor on the response, heat transfer rate q, measured in Watts. The second stage of this experiment consisted of quantifying the test board heating effects of each factor and developing a model with the data through the use of response surface analysis. The oven used for this experiment consists of eight heating zones with two cooling fans (Electrovert Bravo 8105). The experimental results apply solely for this oven.

4.3.1   The Experimental Procedure

The original factorial screening experiment consisted of selecting 3 factors with high and low settings. The factors and settings listed in Table 15 were chosen based on previous empirical results and availability. The experiment consisted of a single replicate 2^3 factorial design with center points.

Table 15: 2³ Factorial Parameters and Settings

Factor	Setting
Oven Temperature	High and Low (130 and 220ºC)
Conveyor Speed	High and Low (11 and 21 in/min)
Convection (blower) Setting	Med High and Med Low Blower Settings (measured in cubic ft./min)

The procedure throughout the experiment consisted of recording temperature profiles on a test vehicle for each experimental condition (See Table 16). The test vehicle (the experimental unit) consisted of a flat plate of ECP plus material with six thermocouples attached diagonally across the plate as shown in Figure 31. A sample profile for this test vehicle is shown in Figure 32. The results from the initial screening experiment were used to detect linear effects and provide information on the existence of possible second order effects (curvature) in the model.

Figure 31: Experimental Unit / Test Vehicle

Table 16: Initial Screening Experiment Oven Settings

Blower (cfh)	Conveyor Speed (in/min)	Oven Tº (ºC)	
0.0482	11.4	130	
0.0642	11.4	130	
0.0482	21.4	130	
0.0562	16.4	175	
0.0562	16.4	175	
0.0562	16.4	175	*
0.0562	16.4	175	*
0.0562	16.4	175	*
0.0562	16.4	175	*
0.0562	16.4	175	*
0.0482	11.4	220	*
0.0642	11.4	220	
0.0482	21.4	220	
0.0642	21.4	220	

*Center points

Ben Salomon
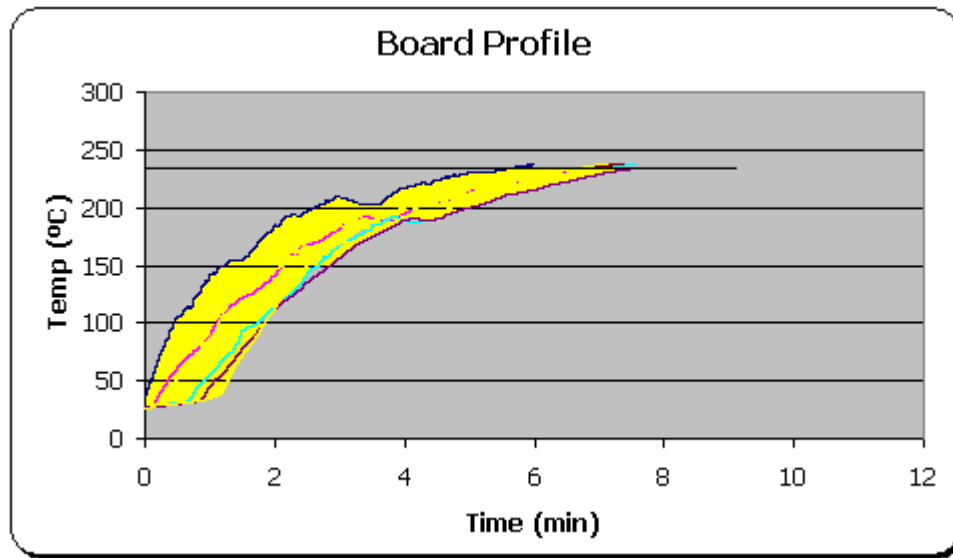
Figure 32: Typical Board Profile showing Experimental Range

The average heat rate response across the experimental unit was measured indirectly by observing the temperature increase in the six thermocouples attached to the board for the range shown in Figure 32 (shaded region of sample profile above).
`

In general, the procedure followed was to calculate the energy increase (Joules) at each thermocouple and dividing this value by the amount of time it took to reach a predetermined point in time. The response, heat rate (Watts) up to this specified time, was measured by use of the lumped capacitance method for transient conduction. See Appendix 1 for an explanation on the method used in this experiment to calculate q, the heat transfer rate.

4.3.2 Experiment Results: Screening Experiment

Results for the factorial portion of this investigation indicates a relatively strong temperature effect and moderate but significant conveyor and convection effects when settings are changed from low to high. These results are summarized in Figure 33.

Ben Salomon

The interaction plots shown in Figure 33 indicate that conveyor and convection effects are greater at higher temperatures. The blower-convection plot also indicates no apparent interaction between convection and conveyor factors and moderate interaction between oven temperature and the other factors. These results are quantified in the ANOVA shown in Table 17.
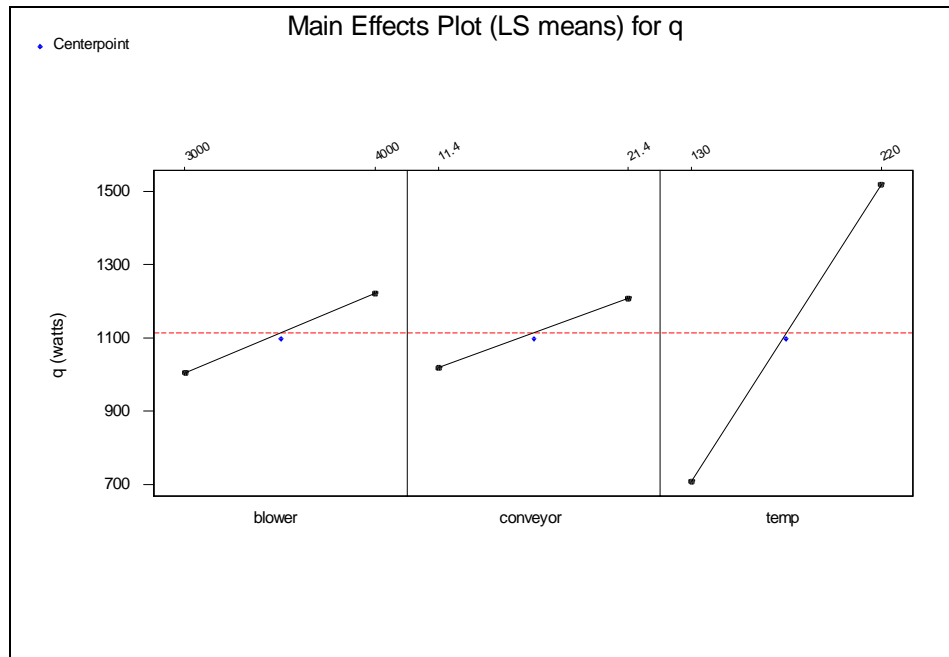
Figure 33:Main Effects Plot for Board Heat q

In general, higher temperatures, faster conveyor speeds and higher blower settings will significantly increase the heat transfer rate at the test board surface. Both conveyor and convection factors interact significantly with oven temperature. Changing blower settings at slow or fast conveyor speeds will not cause a relative difference in the overall heating rate response. Convection and conveyor settings do not interact to cause a significant change in the rate of board heating.
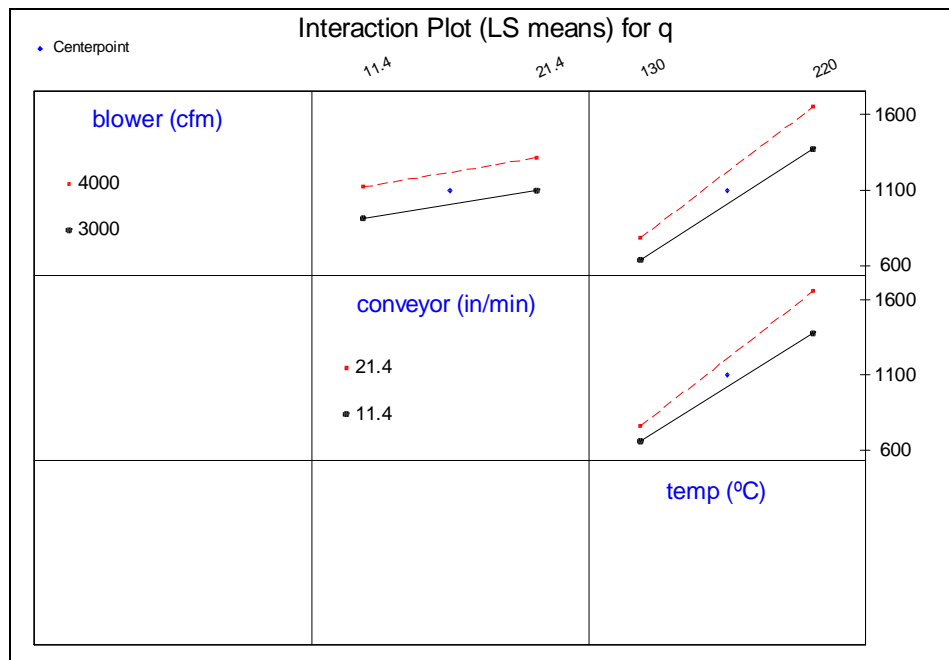
Figure 34: Interaction Plots for Board Heat q

In general, higher temperatures, faster conveyor speeds and higher blower settings will significantly increase the heat transfer rate at the test board surface. Both conveyor and convection factors interact significantly with oven temperature. Changing blower settings at slow or fast conveyor speeds will not cause a relative difference in the overall heating rate response. Convection and conveyor settings do not interact to cause a significant change in the rate of board heating.

The relative significance of each factor is graphically summarized in Figure 35 and with the ANOVA, Table 17. The plots in Figure 35 indicate that Oven Temperature (C), Blower settings (A) and Conveyor speed (B) all have a significant effect on the response at a significance level of alpha = 0.05. The plots also indicate the relative importance of the interactions between conveyor and blower settings with oven temperature. Table 17 shows that three way and curvature effects in this model are not significant within this experimental region.

Table 17: ANOVA Table for Heating Rate Experiment

```
Estimated Effects and Coefficients for q (coded units)
Term                    Effect      Coef    SE Coef      T      P
Constant                           1113.48    14.55   76.54  0.000
blower                  215.15    107.57      14.55    7.39  0.000
conveyor                189.37     94.69      14.55    6.51  0.000
temp                    807.08    403.54      14.55   27.74  0.000
blower*conveyor           4.02      2.01      14.55    0.14  0.894
blower*temp              66.27     33.13      14.55    2.28  0.052
conveyor*temp            89.29     44.64      14.55    3.07  0.015
blower*conveyor*temp     16.56      8.28      14.55    0.57  0.585
Ct Pt                             -14.72      19.99   -0.74  0.483
```

| Analysis of Variance for q (coded units) | | | | | | |
Source	DF	Seq SS	Adj SS	Adj MS	F	P
Main Effects	3	1467068	1467068	489023	288.82	0.000
2-Way Interactions	3	24759	24759	8253	4.87	0.033
3-Way Interactions	1	548	548	548	0.32	0.585
Curvature	1	918	918	918	0.54	0.483
Residual Error	8	13545	13545	1693		
Pure Error	8	13545	13545	1693		
Total	16	1506838				

```
Estimated Coefficients for q using data in uncoded units
Term                       Coef
Constant              -741.00
blower                  0.155434
conveyor               26.4714
temp                    4.78289
blower*conveyor        -0.0120732
blower*temp             0.00026593
conveyor*temp          -0.059117
blower*conveyor*temp    0.000073580
Ct Pt                 -14.7230
```

Ben Salomon

Normal Probability Plot of the Standardized Effects
(response is q, Alpha = .05)

Pareto Chart of the Standardized Effects
(response is q, Alpha = .05)
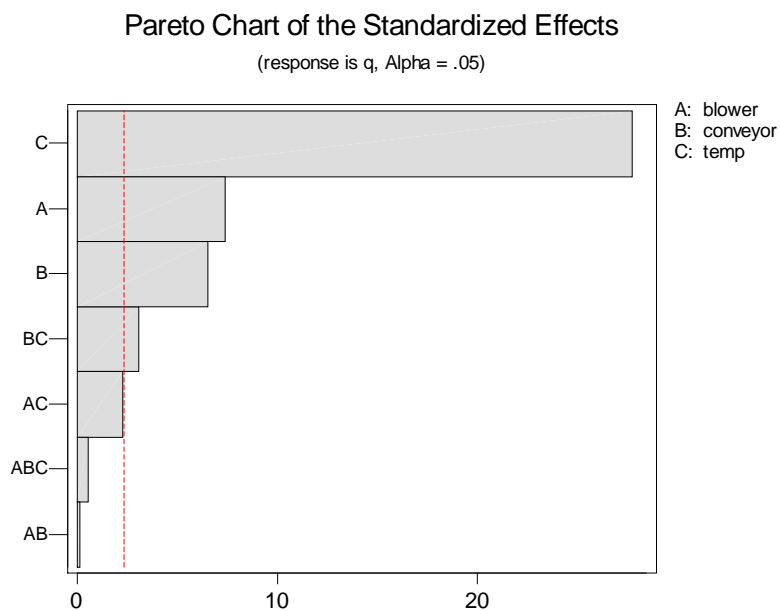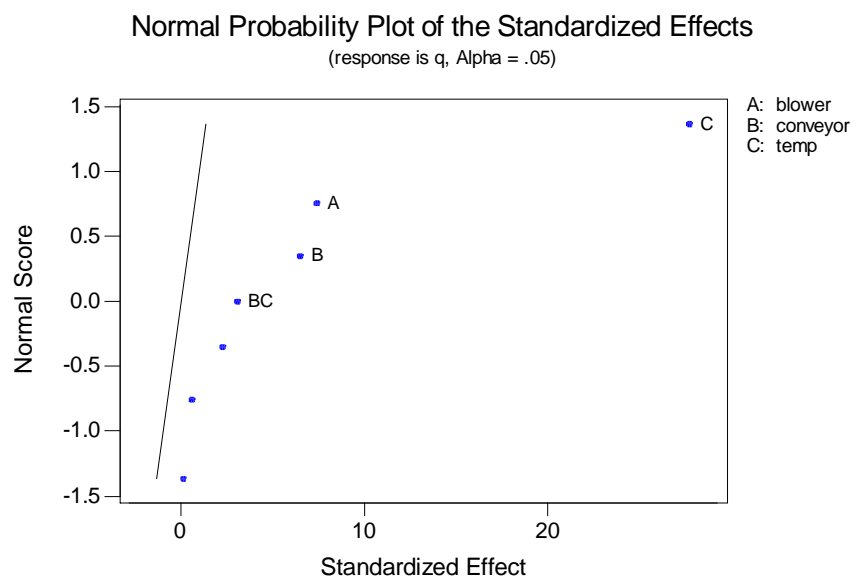
Figure 35: Normal Probability plot and Pareto Comparing Magnitude of Effects

Ben Salomon

A graphical summary of the factorial model is shown in Figure 36. The cube plot indicates that conditions for highest heat transfer rate occur at the highest settings for all factors. This result is consistent, expected and intuitive. With higher settings, the board heating rate is also higher due to convective, temperature and time effects associated with these settings. Also expected is the significance of all main effects. Characterization of heat transfer q (watts) can be summarized by the equation in Table 18, applicable only for the factor space covered by this experiment.

⊕ Centerpoint
▪ Factorial Point

Cube Plot (LS means) for q (watts)

1505.35   1807.34
691.81   828.15
21.4
              1098.8
              ⊕
conveyor (in/min)
1247.27   1508.11
                   220
              temp (ºC)
579.18   740.60
11.4   130
3000   4000
blower
(cfm)
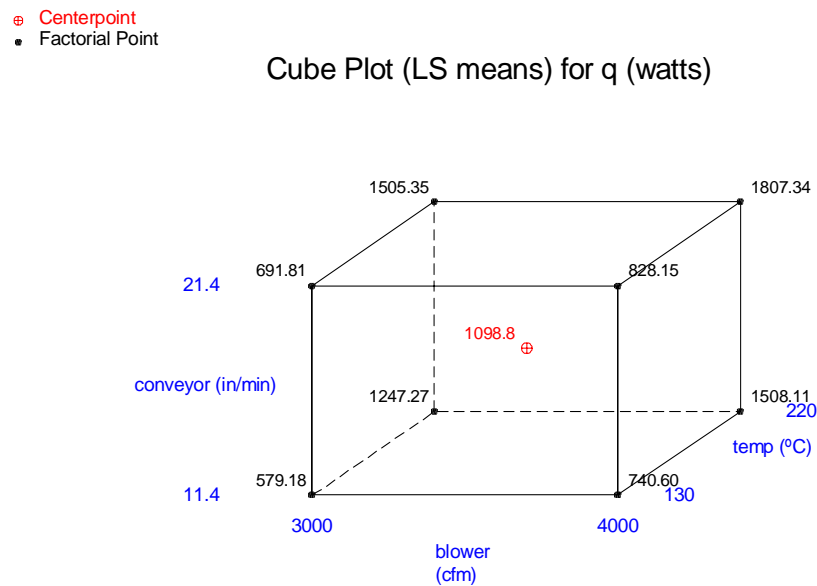
Figure 36: Cube plot for the Factorial Model

Ben Salomon

Table 18: Board heat rate as a function of volumetric flow, transport speed and oven temperature. Linear model.

q = -755.72 + 0.16(A) + 26.47 (B) + 4.78 (C) - 0.06 (BC)

A = Blower Setting (cfm)

B = Conveyor (in/min)

C = Oven Temperature (°C)

q = heat transfer (watts)

4.3.3   Experiment Results: Response Surface

A second order model (a full quadratic) was created using the data from the linear model above and additional data observations listed in Table 19. The response surface model was used to find optimum conditions for oven heat transfer rate and to understand the influence and interaction of each factor within an extended experimental range. The analysis of variance shown in Table 20 indicates that both linear and strong quadratic terms are significant for this extended region and that the fitted surfaces must be an adequate approximation of the true response function (lack of fit > 0.05). The most relevant single factor is temperature, as expected. Both temperature and conveyor have a strong quadratic effect and some interaction occurs between these two factors. Surprisingly, convection is not a significant contributor to heat transfer rate at the board's surface.

Ben Salomon

Table 19: Sample Oven Settings and Response for Full Quadratic Experiment

Blower (cfm for 16 blowers)	Conveyor Speed (in/min)	Oven Tº (ºC)	Observed Response (Watts	
3500	16.4	100	570.605	
3000	11.4	130	579.1826	
4000	11.4	130	740.5985	
3000	21.4	130	691.8097	
4000	21.4	130	828.1474	
3000	16.4	175	1047.678	
4800	16.4	175	1297.993	
3500	3	175	518.6746	
3500	29.8	175	1292.155	
3500	16.4	175	1073.059	*
3500	16.4	175	1063.143	*
3500	16.4	175	1090.134	*
3500	16.4	175	1102.833	*
3500	16.4	175	1155.544	*
3500	16.4	175	1160.369	*
3500	16.4	175	1054.918	*
3500	16.4	175	1058.719	*
3500	16.4	175	1130.062	*
3000	11.4	220	1247.268	
4000	11.4	220	1508.11	
3000	21.4	220	1505.355	
4000	21.4	220	1807.34	
3500	16.4	250	2064.535	

*Center Points

Ben Salomon

Table 20:ANOVA for Central Composite Model

```
Estimated Regression Coefficients for q
Term                      Coef      SE Coef          T       P
Constant                 22.35      990.683      0.023   0.982
BLOWER                    0.26        0.376      0.699   0.497
CONVEYOR                 24.90       32.794      0.759   0.461
TEMP                    -11.14        4.235     -2.632   0.021
BLOWER*BLOWER            -0.00        0.000     -1.109   0.287
CONVEYOR*CONVEYOR        -1.13        0.241     -4.688   0.000
TEMP*TEMP                 0.03        0.007      4.851   0.000
BLOWER*CONVEYOR          0.00        0.008      0.101   0.921
BLOWER*TEMP              0.00        0.001      1.672   0.118
CONVEYOR*TEMP            0.20        0.088      2.253   0.042
S = 56.05       R-Sq = 98.7%     R-Sq(adj) = 97.8%
Analysis of Variance for q
Source                   DF     Seq SS      Adj SS      Adj MS      F       P
Regression                9    3090326     3090326      343370  109.31  0.000
  Linear                  3    2896978       32043       10681    3.40  0.050
  Square                  3     168589      168589       56196   17.89  0.000
  Interaction             3      24759       24759        8253    2.63  0.094
Residual Error           13      40837       40837        3141
  Lack-of-Fit             5      27292       27292        5458    3.22  0.069
  Pure Error              8      13545       13545        1693
Total                    22    3131163
```

The ANOVA in Table 20 also indicates that the quadratic model will probably explain a high percentage (about 97%) of the variability in the data if all displayed terms are included. Overall, linear and quadratic effects in factors temperature and conveyor drive the model. The response surfaces and contour plots for the quadratic model are shown in Figure 37 through 42. By keeping the convection factor constant at 4800 cfm, the highest setting, the heat transfer rate at the board surface is approximated by the equation in Table 21.

Table 21: Heat Transfer equation as a function of conveyor speed and oven temperature

$$q = -1.13(B)^2 + 0.035(C)^2 + 0.2(B)(C) + 28.74(B) - 3.94(C) + 187.47$$

B = conveyor speed (in/min)   C = oven temperature (°C)   q = heat transfer (Watts)

The above equation characterizes the heat transfer rate at the board surface for the conditions and equipment described in this experiment. A comparison of heat transfer rates is possible if this experiment design were replicated for other similar ovens used in this plant (e.g. ovens used for reflow). Heat transfer rate differences among ovens will ultimately depend on the efficiency in oven design, power rating of the heaters and the effectiveness of forced convection blowers.
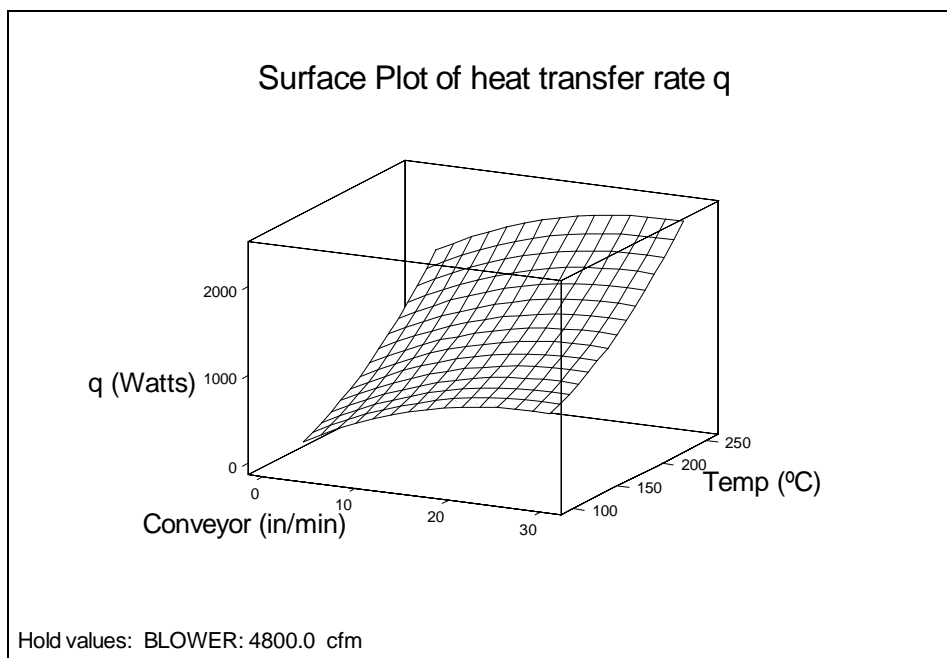
Figure 37: Surface Plot for Board heating rate. Conveyor-Temperature-combination

Ben Salomon
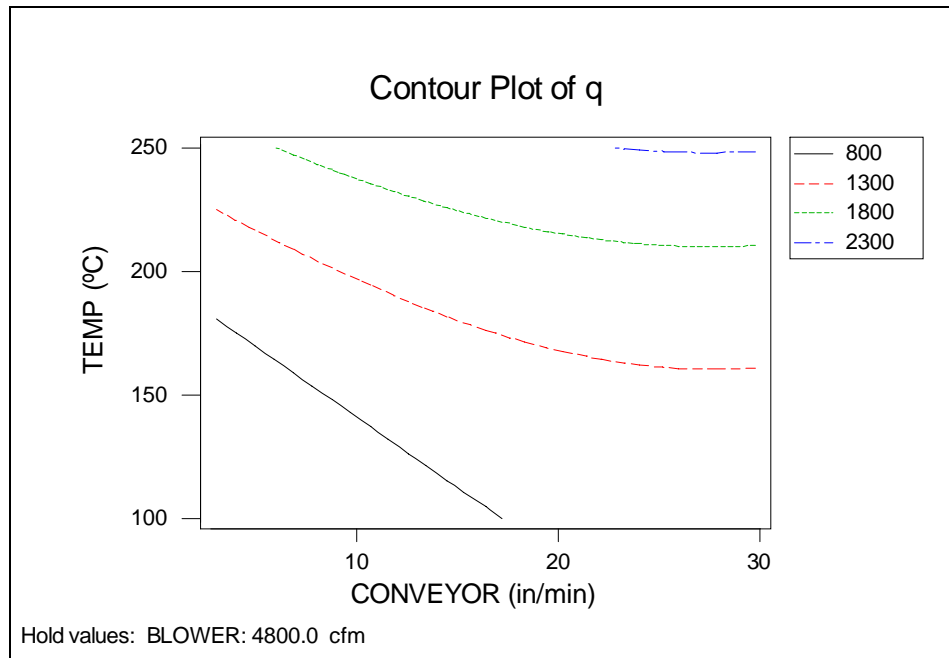
Figure 38: Contour Plot for Board heating rate. Conveyor-Temperature combination
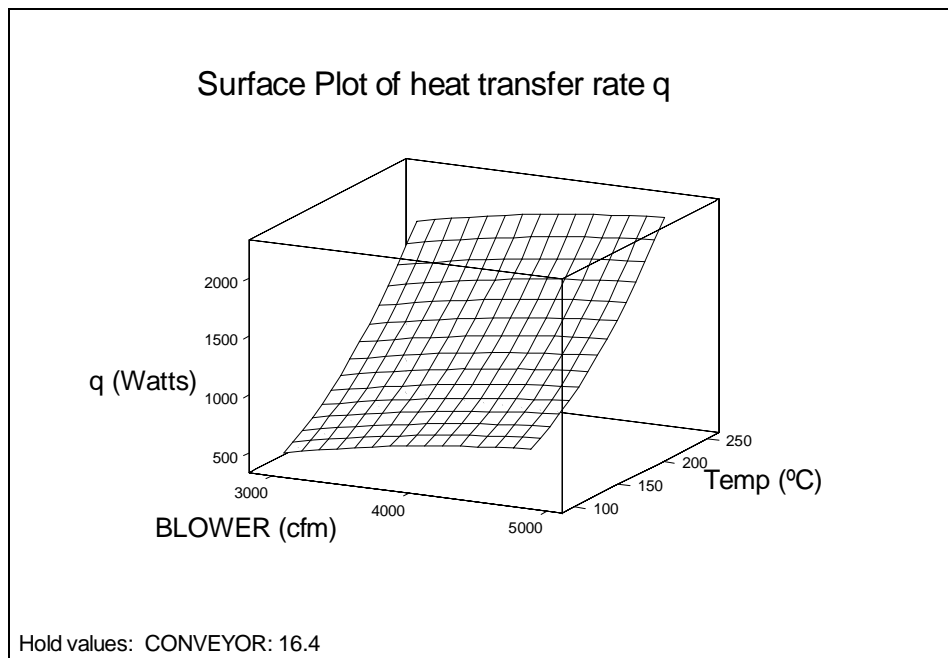
Figure 39:Surface Plot for Board heating rate. Blower-Temperature combination

Ben Salomon
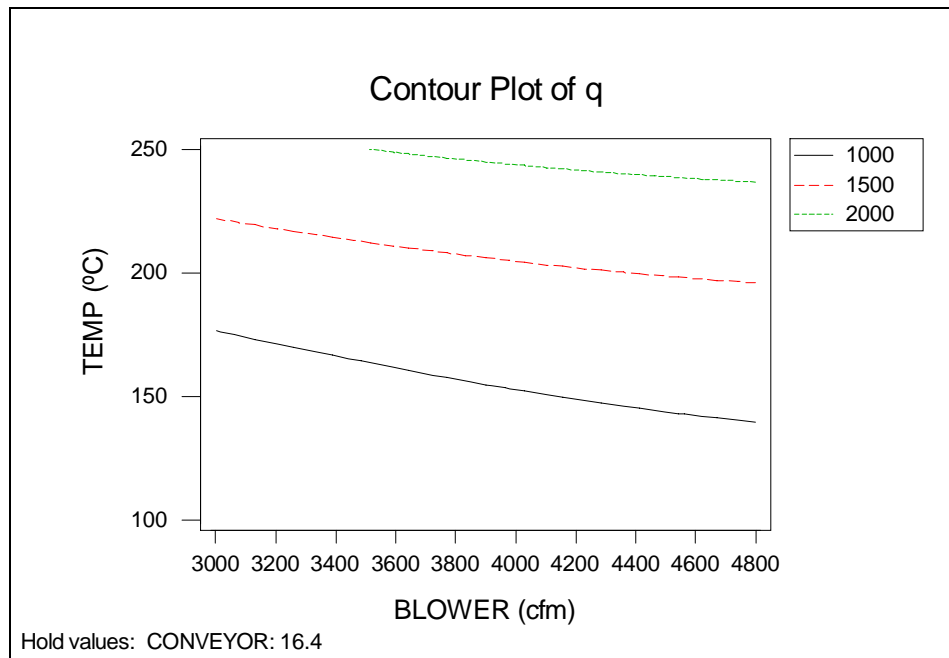
Contour Plot of q

Figure 40: Contour Plot for Board heating rate. Blower-Temperature combination

Surface Plot of q

Figure 41: Surface Plot for Board heating rate. Conveyor-Blower combination

Ben Salomon
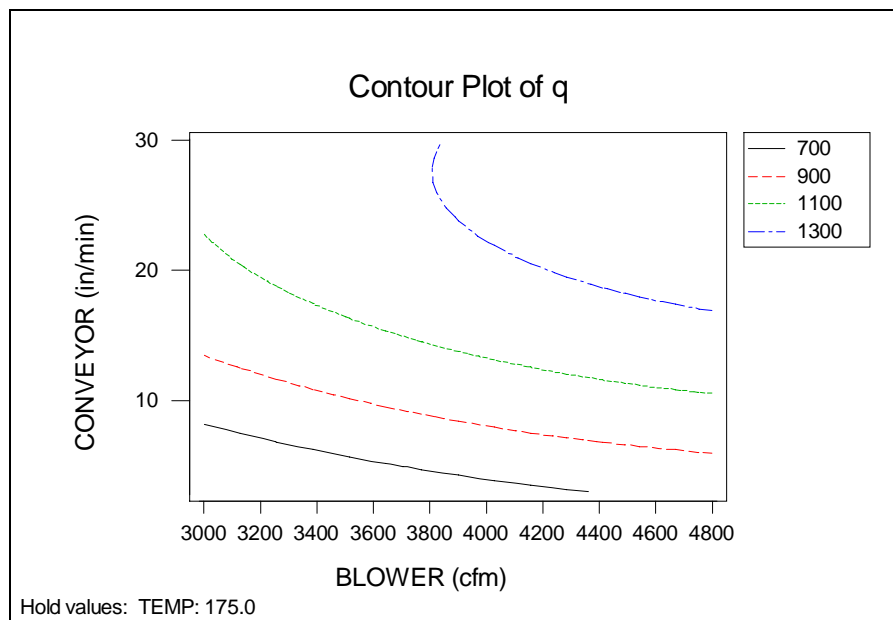
Figure 42: Contour Plot for Board heating rate. Conveyor-Blower combination

Although the linear model gave no indication of curvature effects, the oven experiment was augmented to cover an extended region based on the experimenter's experience and knowledge of the heat transfer mechanisms for this process.   T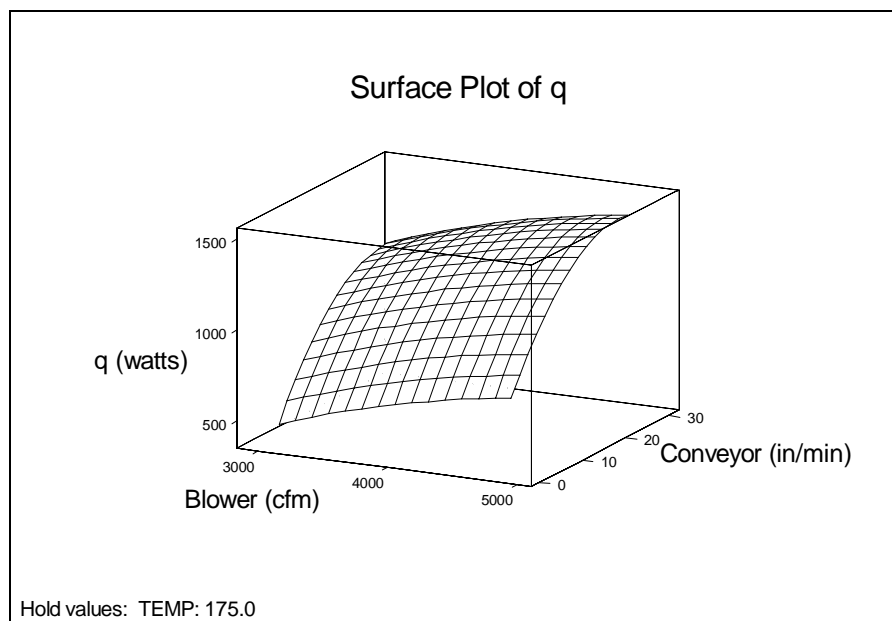he quadratic effects in conveyor and temperature are most likely caused by exponential effects of the fundamental heat transfer rate equation. The convection factor lack of significance in this experiment most likely due to the heat transfer convective coefficient *h* which is strongly temperature and time dependent. Convection effects are probably important in maintaining temperature uniformity throughout the oven. Further analysis in this area is required.

The quadratic model presented in this experiment is barely adequate as the lack of fit tests demonstrates, but suitable as an approximation for the region covered in this characterization. The methods presented here for oven characterization are applicable to other reflow ovens and the calculated parameters, may serve as indices of comparative heating effectiveness.

In closing, higher heat transfer rates do not necessarily prescribe better temperature reflow profiles as shown in Figure 43 where some positive correlation seems to exist between heat transfer rate and temperature dispersion across the board.

Temperature dispersion vs Heat transfer rate
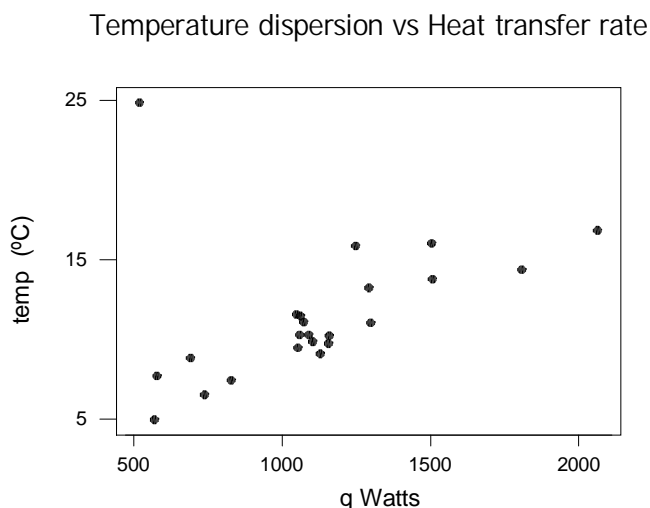
Figure 43: Board Temperature Standard Deviation vs. Board Heat Transfer Rate

Finally, the results presented here apply exclusively for constant oven temperatures and serve only to provide general characterization information as explained above. Further investigations on actual board profiles using actual boards are possible given enough time and resources. In retrospect, replication of each treatment may improve the accuracy of experimental error, and possibly shed more model information. A possible source of error may have been induced by the initial temperature variations T_i at the beginning of each profile. A possible application of the method presented here is in the general characterization and comparison of heat transfer rates of other reflow ovens.

4.4   Underfill Yielded Cost Model

The underfill cost model is based on information gathered from references [27], [28] and [29]. The yielded cost metric is documented in reference [28]. Reference [27] is a good source for understanding board assembly cost modeling for a test/diagnosis/repair process. Reference [29] was used to estimate board yield after repeated rework attempts.

In general, yielded cost is the total cost per board assembly divided by the total yield of the process under consideration. The yielded cost concept as applied to this model can be interpreted as the total cost per board using the test/troubleshooting/repair (TTR underfill) process divided by the final yield. The cost referred here is the total cost per board accrued during the various operations. The final yield is determined by the yield of individual operations, scrap generation, the effectiveness of the test coverage and the possibility of false positives created by the test operation. Thus defined, yielded cost can be interpreted as the manufacturing cost per good board assembly [28].

The basic formula used for the yielded cost metric is,

$$C_{yielded} = \frac{C_{out}}{Y_{out}}$$

This metric quantifies cost and quality. A quick look at this equation indicates the obvious: in order to improve $C_{yielded}$ we must strive to decrease C_{out} and increase Y_{out}. Determining yielded cost will be the model's objective and will be used to compare different rework scenarios. The general approach presented here is to calculate and compare the yielded cost for a fixed number of rework attempts given a defined set of inputs. A spreadsheet (testmodel.xls) was developed to aid with the model's iterations and equations. The sections that follow define the nomenclature

Ben Salomon

and equations for the model, explain how the results were obtained and offer concluding remarks.

4.4.1 The Model

A representation of a test/troubleshooting/repair and underfill process (TTR underfill process) setup is presented in Figure 44.
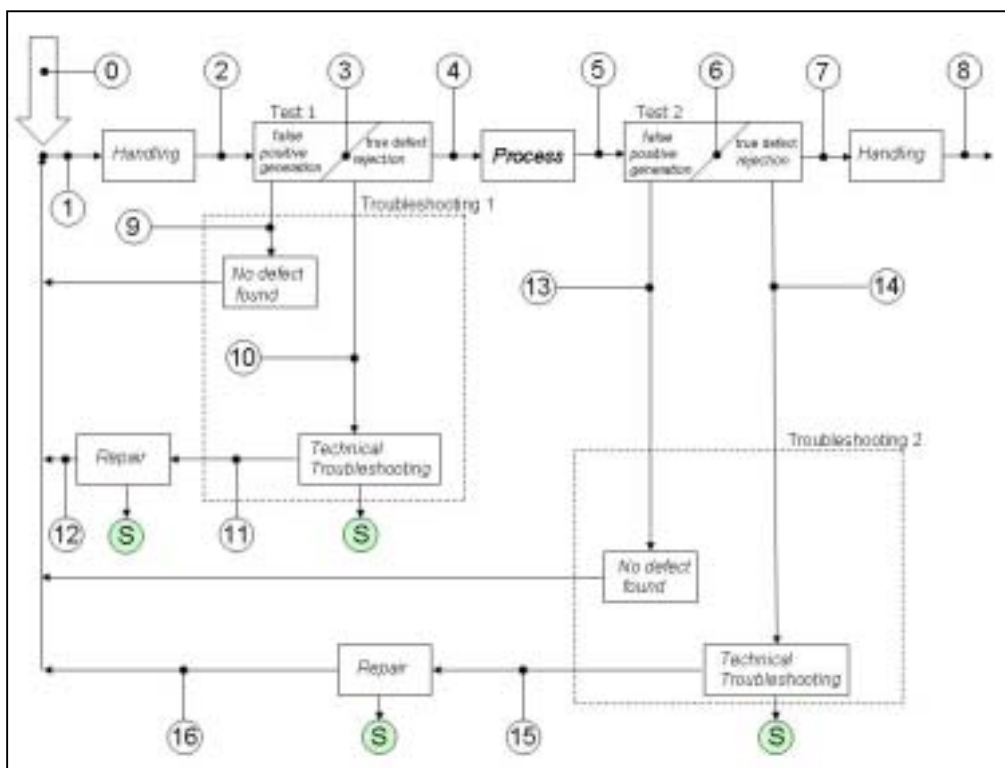
Figure 44: Test/Repair/Troubleshooting underfill schematic

Since the underfill process is embedded between two test operations, the test yields and rework operations must be accounted for in order to understand the cost and yield relevance of an underfill process.

All boards, new or repaired, enter the process at step1. The process step between the first tester (Test 1) and the second tester (Test 2) represents an intermediate operation such as an underfill process. The effect of an underfill operation on yielded cost is modeled by varying the fraction of boards deemed reworkable in the troubleshooting step. The possible generation of scrap caused by the inability to repair an underfilled component and the impact of an underfill process between the two test operations will be considered also.

The required inputs are listed in Table 22. Nomenclature for the algebraic count of boards and the yield for various steps are shown in Table 23. The notation corresponds with that used in the spreadsheet testmodel.xls. Upstream processes before the TTR underfill operation are represented by the large input arrow at 0 in the schematic depicted by Figure 38 and bring inputs C_{in} and Y_{in} into the model.

Equations (1) through (6) give the accumulated costs at each cost center.

$$C_1 = \sum_{i=0}^{n} (Cin_i + Ctest1 + Cprocess + Ctest2_i) Nout_i \tag{1}$$

$$C_2 = \sum_{i=1}^{n} (Cin_{i-1} + Ctest1 + Ctrb1) Nstrb1_{i-1} \tag{2}$$

$$C_3 = \sum_{i=1}^{n} (Cin_{i-1} + Ctest1 + Cpro + Ctest2 + Ctrb2) Nstrb2_{i-1} \tag{3}$$

$$C_4 = \sum_{i=1}^{n} (Cin_{i-1} + Ctest1 + Ctrb1 + Crw1) Nsrw1_{i-1} \tag{4}$$

$$C_5 = \sum_{i=1}^{n} (Cin_{i-1} + Ctest1 + Cpro + Ctest2 + Ctrb2 + Crw2) Nsrw2_{i-1} \tag{5}$$

$$C_6 = (Cin_n + Ctest1)(Nfp1_n + Nd1_n) + (Cin_n + Ctest1 + Cpro2 + Ctest2)(Nfp2_n + Nd2_n)$$

$$\tag{6}$$

All boards leaving the TTR underfill process will incur the cost given in (1). Boards passing through troubleshooting operations will accumulate the scrap costs given in (2) and (3). The rework processes contribute scrap costs given in (4) and (5). Finally, the cost of all boards rejected in the last test cycle is given in (6). No costs are incurred at the troubleshooting or rework stations when no rework is allowed.

Table 22: Required Inputs for the TTR underfill model

Cin	Cost per board when entering process ($/bd).
Ctest1	Cost of test1 per board ($/bd).
Ctest2	Cost of test2 per board ($/bd).
Cprocess	Cost per board of underfill process between tests ($/bd).
Ctrb1	Cost of troubleshooting operation1 per board ($/bd).
Ctrb1	Cost of troubleshooting operation 2 per board ($/bd).
Crw1	Cost of rework operation 1 per board ($/bd).
Crw2	Cost of rework operation 2 per board ($/bd).
fd1	Fraction of boards determined repairable by troubleshooting1 process. A (1-fd) fraction is scrapped at troubleshooting station.
fd2	Fraction of boards determined repairable by troubleshooting2.
fr1	Actual reworked fraction of boards at rework station1. A (1-fr) fraction is scrapped at repair station.
fr2	Actual reworked fraction of boards at rework station 2.
tc1	Test coverage fraction at test1.
tc2	Test coverage fraction at test2.
fp1	False positive fraction created at test1.
fp2	False positive fraction created at test2.
Yin	Board yield entering the TTR underfill process.
Yh1, Yh2	Yield of handling processes during TTR UNDERFILL operations.
Ypro	Yield of process between test1 and test2.
Yrw1	Yield of rework operation1.
Yrw2	Yield of rework operation 2.
Nin	Number of boards entering TTR underfill process.

Ben Salomon

Table 23: Yield and Board Count Nomenclature at locations shown in Figure 38

At location	Yield	Board Count	Comment
0	Yin_0	Nin_0	Model input
1	Yin_i	Nin_i	Input from 0 or rework process.
2	$(Yh1)(Yin_i)$	Same as 1	Yield after first handling
3	Yfp1	Nafter_fp1	State after false positives are created at test1
4	Yout_t1	Nout_t1	State leaving test1
5	(Yout_t1)(Ypro)	Same as 4	Yield after intermediate process
6	Yfp2	Nafter fp2	State after false positives are created at test2
7	Yout_t2	Nout_t2	State after leaving test2
8	Yout	Nout	Output state
9	n/a	Nfp1	False positive board count by test1
10	n/a	Nd1	Reject count from test1 with true defects
11	n/a	Nrw1	Board count entering rework station 1(rew1)
12	n/a	Nrout1	Board count leaving rew1
13	n/a	Nfp2	False positive board count by test2
14	n/a	Nd2	Reject count from test2 with true defects
15	n/a	Nrw2	Board count entering rework station 2(rew2)
16	n/a	Nrout2	Board count leaving rew2
S at troub1	n/a	Nstrb1	Scrap generated at troubleshooting station 1 (troub1)
S at troub2	n/a	Nstrb2	Scrap at troub2
S at rew1	n/a	Nsrw1	Scrap at rew1
S at rew1	n/a	Nsrw1	Scrap at rew2

Equations (7) through (16) are model equations for the first tester and are used in the spreadsheet testmodel.xls. Refer to Figure 44 for designated locations. Test 2 equations are similar to Test 1 equations.

At locations 3 and 9,

$$Nfp1_i = Nin_i * fp1 * Yin_i * Yh1 \tag{7}$$

$$Nafterfp1_i = Nin_i(1 - fp1 * Yin_i * Yh1) \tag{8}$$

$$Yfp1_i = \frac{(1 - fp1)Yin_i * Yh1}{1 - fp1 * Yin_i * Yh1} \tag{9}$$

At locations 4 and 10,

$$Nout\_t1_i = Nafterfp1_i(Yfp1_i)^{tc1} \tag{10}$$

$$Yout\_t1_i = Yfp1_i^{(1-tc1)} \tag{11}$$

$$Nd1_i = Nafterfp1_i(1 - Yfp1_i^{tc1}) \tag{12}$$

At locations 11 and 12,

$$Nrw1_i = fd1(Nd1_i) \tag{13}$$

$$Nstrb1_i = (1 - fd1)(Nd1_i) \tag{14}$$

$$Nrout1_i = fr1(Nrew1_i) \tag{15}$$

$$Nsrw1_i = (1 - fr1)(Nrew1_i) \tag{16}$$

Equations (7), (8) express the board count for falsely rejected boards and the number of boards available after deducting false positives. Equation (10) expresses the output after testing as a function of the false positive and test coverage fraction. The quantity of boards that are rejected with true defects is given by (12). The

quantity of boards passing through and scrapped by the troubleshooting and rework operations is given in (13) through (16).

The effect of false positives on yield is given by (9). The derivation of this yield is found in [26]. Equation (11) expresses the output yield of boards leaving a test operation and is based on the Williams-Brown equation [30]. The equations in (17), (18) and (19) increment the iterations for Nin, Yin and Cin reentering the TTR underfill process from troubleshooting and repair operations of both test centers. Count increment occurs after repair.

$$Nin_i = \begin{cases} Nin & \text{when } i = 0 \\ Nfp1_{(i-1)} + Nrout1_{(i-1)} + Nfp2_{(i-1)} + Nrout2_{(i-1)} & \text{when } i > 0 \end{cases}$$

(17)

$$Yin_i = \begin{cases} Yin & \text{when } i = 0 \\ \dfrac{Nfp1_{(i-1)} + (Yrew1)(Nrout1_{(i-1)}) + Nfp2_{(i-1)} + (Yrew2)(Nrout2_{(i-1)})}{Nin_i} & \text{when } i > 0 \end{cases}$$

(18)

$$Cin_i = \begin{cases} Cin & \text{when } i = 0 \\ \dfrac{(Cin_{(i-1)} + Ctest1 + Ctrb1)Nfp1_{(i-1)} + (Cin_{(i-1)} + Ctest1 + Ctrb1 + Crw1)Nrout1_{(i-1)}}{Nin_i} \\ + \dfrac{(Cin_{(i-1)} + Ctest1 + Cpro + Ctest2 + Ctrb2)Nfp1_{(i-1)}}{Nin_i} \\ + \dfrac{(Cin_{(i-1)} + Ctest1 + Cpro + Ctest2 + Ctrb2 + Crw2)Nrout2_{(i-1)}}{Nin_i} & \text{when } i > 0 \end{cases}$$

(19)

The number of boards reentering the TTR underfill process (17) is the sum of the all repair and false positives generated from either test center. The new Yin (18) can be interpreted as the sum of all good boards reentering the process divided by the total number of boards that reenter. In reality, Yrew1 and Yrew2 will change as each repair cycle improves Nrout1 and Nrout2 boards. A method to model this improvement is documented in [29] and [27]. The repair process will also probably

deteriorate a proportion of Nrout1 and Nrout2 boards that will probably not be detected by either test center.

The cost per board reentering the TTR underfill process (19) is found by proportionately distributing the costs between the number of test-rejected boards that do not have defects (Nfp1 and Nfp2 no-trouble-founds) and those that have been reworked (Nrout1 and Nrout2).

The total number of boards leaving the TTR underfill process is given by (20),

$$Nout = \sum_{i=0}^{n} Nout_i \tag{20}$$

where $Nout_i = Nout\_t2_i$.

The output yield (21),

$$Yout = \frac{Yh2 \sum_{i=0}^{n} Nout\_t2_i * Yout\_t2_i}{Nout} \tag{21}$$

where $Yh2(Nout\_t2_i * Yout\_t2_i)$ is the number of defect free boards leaving the TTR underfill process after each cycle.

The accumulated cost per board (22) is the sum of the costs (1) through (6) divided the total number of boards leaving the TTR underfill process.

$$Cout = \frac{\sum_{j=1}^{6} C_j}{Nout} \tag{22}$$

The yielded cost metric (23) was defined at the beginning of this memo [2].

$$C_{yielded} = \frac{C_{out}}{Y_{out}} \tag{23}$$

Ben Salomon

4.4.2   Underfill effect on Cyield

Partial or full underfill modeling: Assuming an underfill process is required, the effect of partial or full underfill on Cyield can be modeled by changing the fraction of boards determined to be repaired at test 2 (*fd2*) to a value between 0 (no repair possible after test 2) and 1 (rework possible for all boards after test 2).

Figure 45 illustrates the effect of underfill cost per board and the yield of the underfill process on Cyield for a given set of inputs listed in Table 24. The plot demonstrates that an underfill process will increase Cyield and that the Cyield metric is proportionally more sensitive to changes in process yield than to process cost.

No underfill process: If the underfill is not required, the underfill cost per board will be negligible and the underfill process yield will approach 1 (Cpro =0 and Ypro =1). For this limiting case and for the other given set of inputs listed in Table 24, Cyield (the cost of fabricating a defect-free board) will minimize to dollar value of $330.91.

The model was used to show for that for low cost / high yield rework processes, repair could be an option to improve the Cyield metric. Repair is not an option where high cost / low yield repair operations offset the benefits of salvaging defective board assemblies. The model does not consider the effect of board volume on rework processes. From a manufacturing perspective, the assumption that rework cost is independent of board assembly volume will not hold for lower incoming yields as queuing and inventory overwhelm rework and troubleshooting centers.

From Figure 45, an underfill operation will always impact the C_{yield} metric. The underfill process yield must be given special attention as scrap generated after the board assembly has accumulated costs can significantly affect the C_{yield} metric.

Ben Salomon

Table 24: Inputs for TTR underfill model varying underfill Cost (Cpro) and underfill Yield (Ypro)

Cin	250
Ctest1	25
Ctest2	30
Cpro	varies
Ctrb1	45
Ctrb2	40
Crw1	30
Crw2	35
tc1	0.99
tc2	0.98
fd1	1
fd2	0
fr1	0.8
fr2	.8
fp1	0.015
fp2	0.01
Yin	0.99
Yh1	0.98
Ypro	varies
Yrw1	.95
Yrw2	.98
Yh2	0.97
Nin	1000

Ben Salomon
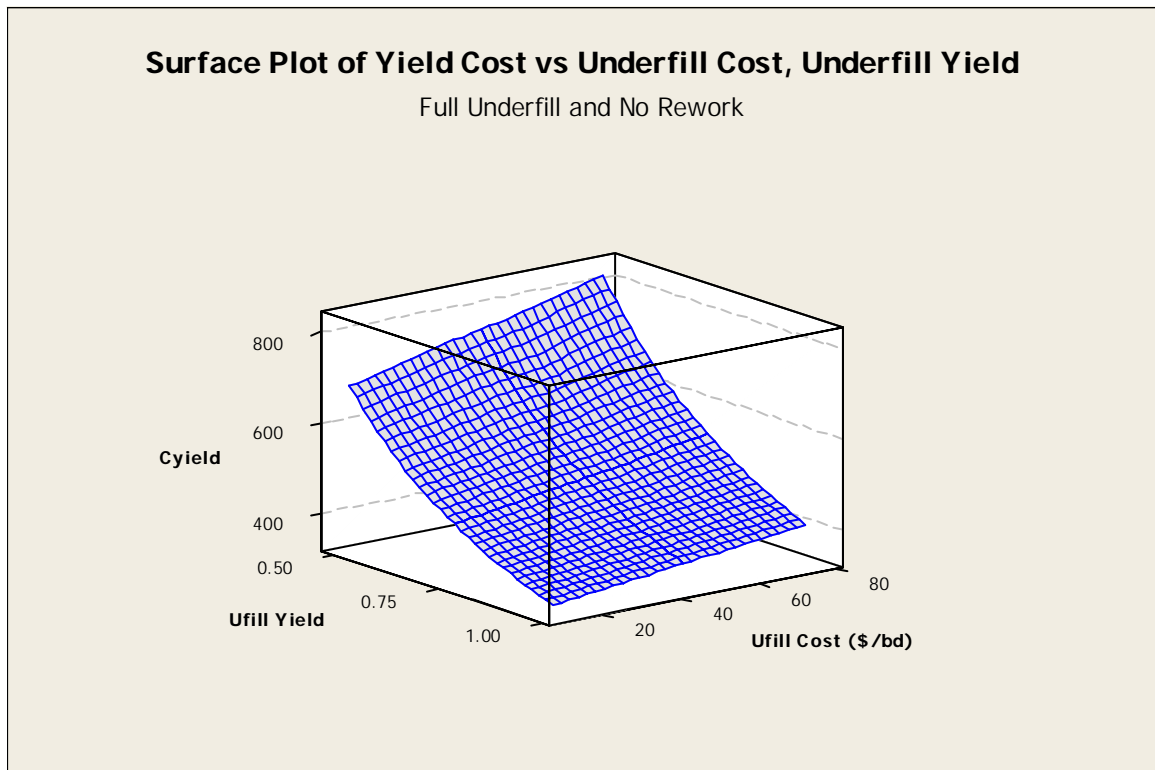
Figure 46: Underfill Process influence on Yield Cost

5 CONCLUSION

The project's practical approach is targeted towards a production environment where results and quick decisions are required on a daily basis. The tools used in this project are supported by a theoretical framework. The conclusions presented in this project are applicable to similar materials and processes.

The underfill process development presented here focused on simple techniques that can be deployed on the production floor. The acceptability criteria that were developed are based on the framework of experiments and statistical analysis. The project established a simple method for underfill inspection based on analysis and rigorous characterization. Correct underfill process deployment was presented from a general perspective and focused on materials, processes and equipment. The main conclusion drawn from the implementation of an underfill process is that successful implementation of an underfill process requires the close collaboration of design, process and equipment.

Underfill curing equipment was also analyzed and presented here. The importance of the analysis is based on the fact that no two ovens are alike and that underfill curing and processing may benefit from high efficiency ovens. The analysis presented here is especially relevant for the process engineer when attempting to choose the correct underfill equipment required for implementation.

The underfill cost model presented in this project provides a consistent and systematic method of quantifying the cost impact of different test/rework and underfill strategies. As with any modeling and prediction method the validity of the results will depend on reliable input data. Whether rework is possible or not or whether rework is economically viable considering other financial information not presented here are questions beyond the scope of this investigation. An attempt was

made to present the available information using a graphical approach in order to understand the relationship between the numerous variables accounted for in this model. Further investigation considering volume-sensitive effects on the underfill process may provide greater detail to the cost model.

6 APPENDICES

6.1 Appendix 1: Lumped Capacitance Method

The method used to approximate the heat transfer rate is based on the lumped capacitance method for transient conduction [22]. Equation 6.1 is the basic energy balance interpretation of this approach where h is the convection heat transfer coefficient, A_s is the surface area of the board, T_{surr} is the oven temperature, ρV the mass of the board, c the specific heat of the board and the derivative term is the rate of temperature change with respect to time.

Equation 6.1: Energy balance equation for Lumped Capacitance method

$$-h(A_s)(T - T_{surr}) = \rho V c \frac{d}{dt} T$$

The total energy transfer up to some time t is given by equation 6.2, where Q is the total energy in Joules, θ_i is defined as the temperature difference between the oven temperature and the initial board temperature ($T_i - T_{surr}$). The time constant τ is defined in equation 6.3 as the response in time of the solid to changes in its thermal environment.

Equation 6.2: Total Energy Transfer

$$Q = \rho V c \theta_i (1 - e^{-t/\tau})$$

Equation 6.3: Thermal Time constant

$$\tau = (1/hA_s)(\rho V c) = R_t C_t$$

Ben Salomon

R_t is the resistance to convection heat transfer and C_t is the lumped thermal capacitance of the solid. This model is analogous an RC circuit.

The thermal time constant was found by calculating 0.3679 of the transient temperature (the y axis in Figure 47) response as shown in Figure 41, representing 0.63 decay in the exponential model. The time constant was easily found for all six thermocouples attached to the test board for every profile.

Table 25 lists the average time constants for all the experimental runs used for this experiment. The heat transfer rate up to a time t was found by using these time constants in equation 6.4. The heat transfer value was calculated up to $t = \tau$ minutes in order to maintain consistency throughout the experiment for all profiles.

Equation 6.4: Heat Transfer equation for Lumped Capacitance

$$q = \rho V c \theta_i (1 - e^{-t/\tau}) / t$$
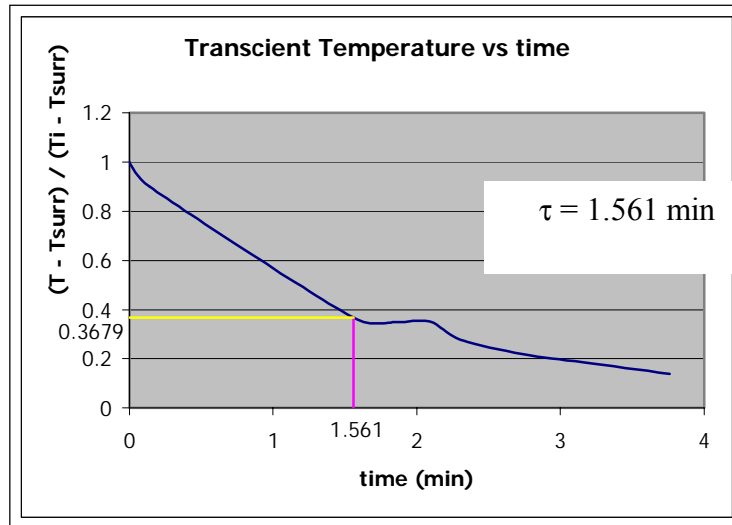
Figure 47: Example of a Transient Temperature Response for a Sample Profile

Ben Salomon

Table 25: Time Constants for all Profiles run in Underfill Curing Oven Experiment

| Convection	Conveyor	Profile	Time Constant (sec)
3500	16.4	100	165.54
3000	11.4	130	239.484
4000	11.4	130	187.81
3000	21.4	130	196.54
4000	21.4	130	154.64
3000	16.4	175	191.68
4800	16.4	175	159.54
3500	3	175	383.25
3500	29.8	175	159.3
3500	16.4	175	192.32
3500	16.4	175	176.21
3500	16.4	175	171.56
3500	16.4	175	176.48
3500	16.4	175	163.61
3500	16.4	175	168.06
3500	16.4	175	184.33
3500	16.4	175	179.57
3500	16.4	175	172.69
3000	11.4	220	208.89
4000	11.4	220	179.06
3000	21.4	220	184.42
4000	21.4	220	148.21
3500	16.4	250	158.15

6.2   Appendix 2: Residual Analysis for Underfill Dispensing Experiment

Model adequacy for the underfill dispensing screening experiment is summarized in Figure 48. The graphs do not indicate a gross deviation from normality (p value > 0.05)) or a problem with the variance of the observations. There is a hint of decreasing residual values as the experiment progressed. This may be due to a change in skill of the experimenter over time. Figure 49 indicates that the data does not provide enough evidence to claim that the measurements in this experiment have unequal variances. In summary, there is no definite indication of problems with the basic experimental assumptions.
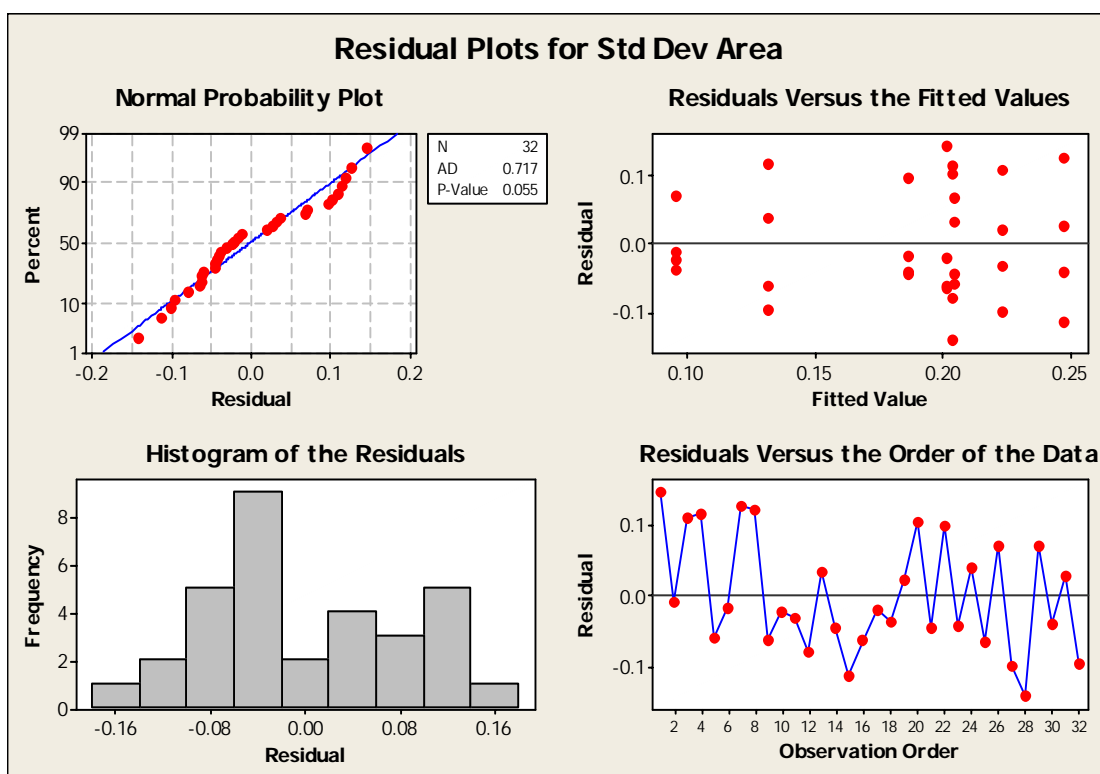
*Figure 48: Residual Analysis for Oven Experiment*
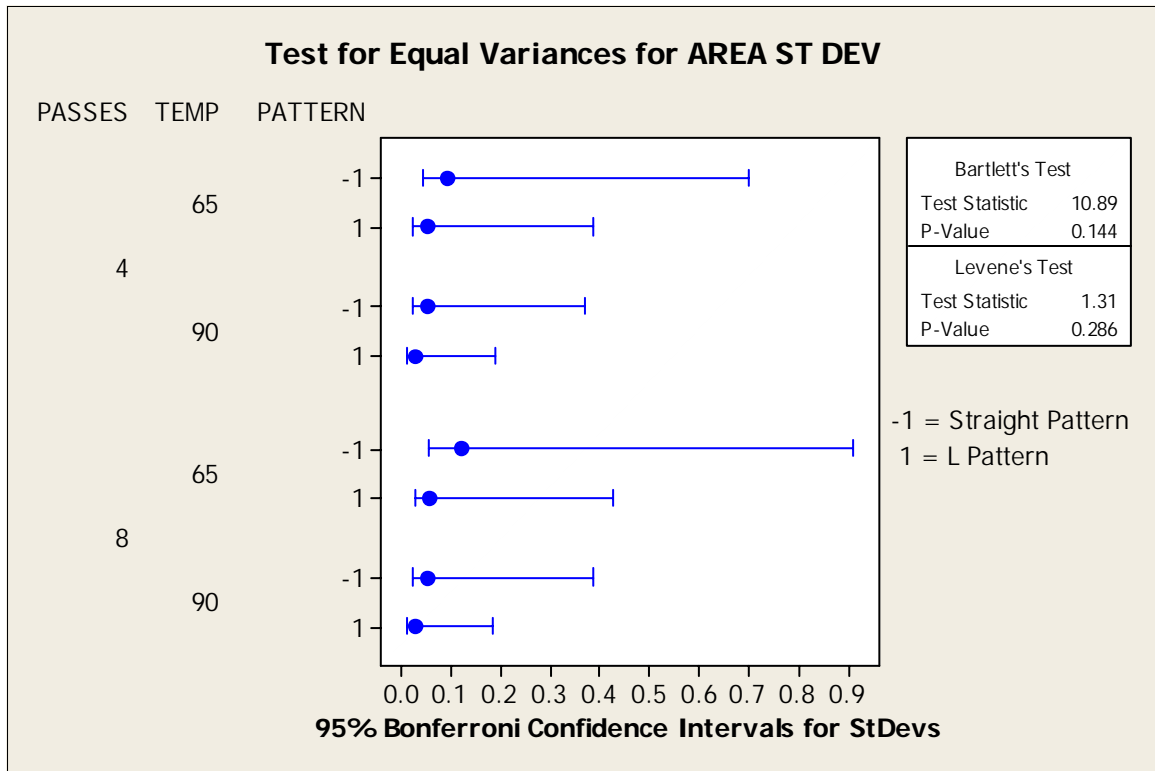
Figure 49: Equal Variances Test for Underfill Screening Dispensing Experiment

6.3   Appendix 3: Residual Analysis for Quadratic Oven Experiment

Residual analysis for the quadratic portion of the oven experiment indicates that the residuals do not severely violate the normality assumption although their distribution indicates a slight skew to the left. The overall conclusion from the summary presented in Figure 50 and Figure 51 is that there is no reason to suspect a gross violation of the basic experimental assumptions.
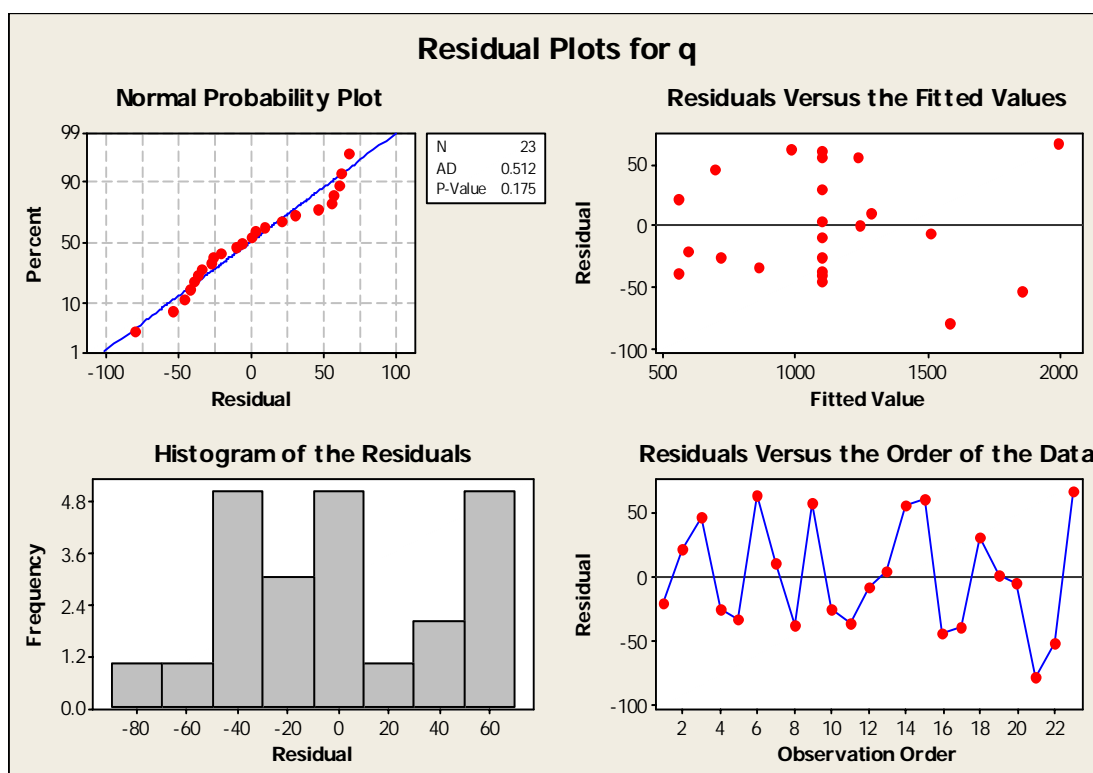
Figure 50: Residual Plots for Underfill Dispensing Screening Experiment

Ben Salomon
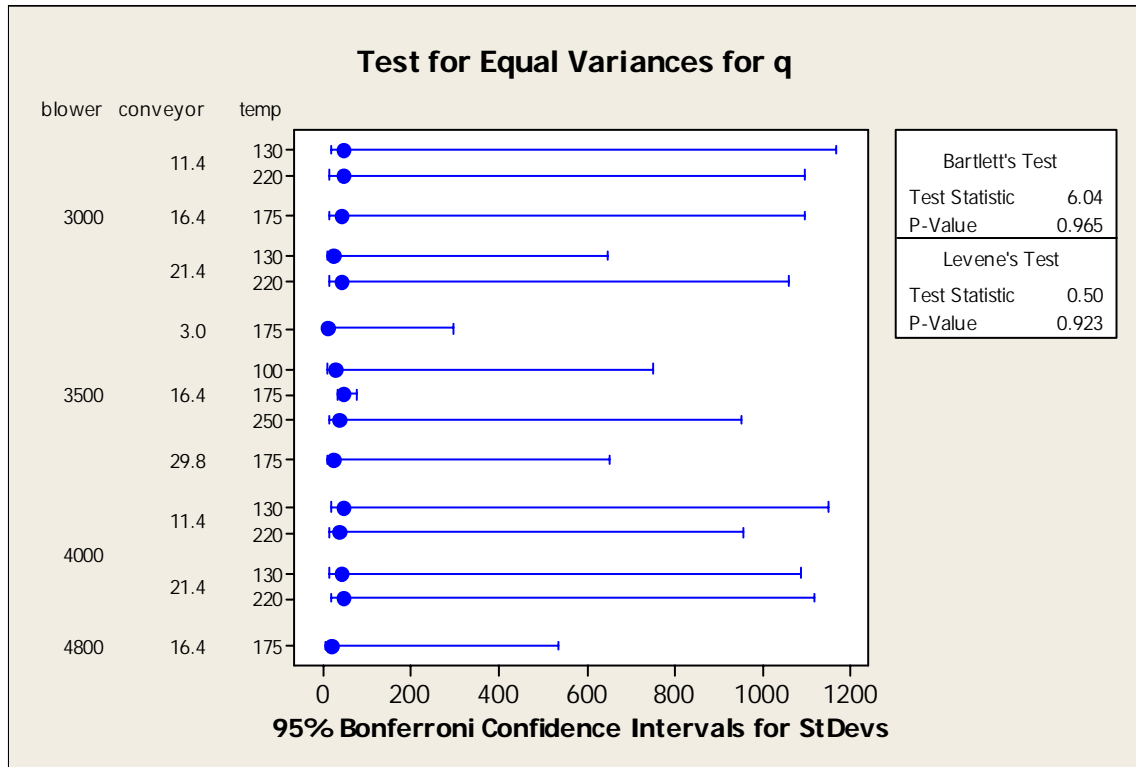
Figure 51: Test for Equal Variances for q

7 BIBLIOGRAPHY

[1]   Schneider, J. *"Improved reliability with underfilled area array packages"*. Polymers and Adhesives in Microelectronics and Photonics. First International IEEE Conference on, 21-24 October, 2001.

[2]   Schneider, J. *"Process Guideline for CSP/BGA Underfills on Board Assembly Level"*. Loctite Research, Development & Engineering. August, 2004

[3]   Doba, T. *"Current Underfills for CSP and BGA"*. Electronic Materials and Packaging. December, 2003

[4]   Haiwei Peng, et al. *"Underfilling fine pitch BGA's"*. Electronic Packaging Manufacturing, October, 2001

[5]   Toleno, B. *"Processing and Reliability of Corner-bonded CSPs"*. IEEE/CPM/SEMI International Electronics Manufacturing Technology Symposium". March, 2003

[6]   Pyland, J. et al. *"Does Underfilling Enhance BGA Reliability?"* Electronics Packaging Technology Conference. December 2000

[7]   Burnette, T. et al. *"Underfilled BGA's for ceramic BGA packages and board-level reliability"* Electronics Components and Technology Conference, May 2000

[8]   Loctite Research, Development and Engineering, *"Application Guidelines for Loctite Underfill Encapsulants"*. Loctite Technical Paper.
http://www.loctite.com/pdf/Application_Guidelines_for_Loctite_Underfill_Encapsulants.pdf

[9]   A.Lewis, C.Ness, B.Verrilli, *"Controlling Fillet Size in Underfill Process"*. Asymtek Archived Articles & Papers.

www.asymtek.com/news/articles/999_02_asymtek_controllingfilletsize.pdf

[10]   G.Carson, M.Edwards, *"Factors Affecting Voiding in Underfilled Flip Chip Assemblies"*. Loctite Research, Development and Engineering. Loctite Technical Paper.

www.loctite.com/pdf/FactorsAffectingVoiding.pdf

[11]   E.Fisher,   *"Loctite   Microelectronic   Products: -40ºC Shipping/Handling/Storage Guide"* Loctite Research, Development and Engineering, Loctite Technical Paper. http://www.loctite.com/pdf/minus40shipping.pdf

[12]   A.Lewis, et al. "Dispensing Requirements for Automating the Underfill Process", Asymtek Technical Document.

http://www.asymtek.com/news/articles/1997_07_flexcon_underfill.pdf

[13]   YewChoon Chia et al. Electronics Packaging Manufacturing, IEEE Transactions, Volume: 26, Issue: 3 , July 2003 Pages: 205 – 210

[14]   Wen-Bin Young, et al; *"The effect of solder bump pitch on the underfill flow"* Advanced Packaging, IEEE Transactions Volume: 25 , Issue: 4 , Nov. 2002 Pages:537 – 542

[15]   C.Huang, K.Srigari, P.Borgesen, *"The Optimization of Underfill Dispensing Process in Flip Chip Assembly"*, Proceedings of the 4th Annual International Conference on Industrial Engineering Theory, Applications and Practice, San Antonio, Texas, November 17-20, 1999.

[16]   D.Peters, *"Mako-Pegasus DRAM Round 3 Power Cycling Report (OSP PC Boards, Impact of Underfill Quality)"* Internal Memo, Hewlett-Packard Company, Business Critical Systems January 17, 2003.

[17]   Taylor, J., et al. "*Solder Joint Reliability Testing of Back-to-Back Assembled BGA Components"*, Taylor, Joyce E.S. and Peters, David W., Proceedings 2002 International Symposium on Microelectronics, International Microelectronics and Packaging Society, pp. 691-696.

[18]   Davidson, D.; Lehmann, G.L.; Cotts, E.J.; *"Effect of geometric surface features on void formation: application to the underfill process"* Electronic Components and Technology Conference, 2002. Proceedings. 52nd, 28-31 May 2002 Pages:1411 – 1418.

[19]   Zhang Fan, et al. *"An investigation into curing behavior and kinetics of underfills for flip chip packages"*. Electronic Materials and Packaging, 2000. (EMAP 2000). International Symposium on, 30 Nov.-2 Dec. 2000, Pages: 313 – 318.

[20]   Cheong, Y.W. et al. *"Effect of underfill staging time on fillet depression"*. Electronics Manufacturing Technology Symposium, 2002. IEMT 2002. 27th Annual IEEE/SEMI International, 17-18 July 2002. Pages: 94 – 96

[21] Yan Tee, Mayhuan Lim, Stephen Pan, Patrick Lam, and Zhaowei Zhong , *"Design Analysis of TFBGA with Customized Solder Joint Fatigue Model"* STMicroelectronics & Optimal Corporation Research. http://www.optimalcorp.com/Support/E-TFBGA1.pdf

[22]   Incropera and Dewitt, *"Fundamentals of Heat Transfer",* Wiley, New York, 1981.

[23]   Montgomery, *"Design and Analysis of Experiments"*, Wiley, New York, 1997.

[24]   Montgomery and Peck, *"Introduction to Multiple Regression"*, Wiley, New York, 2003.

[25]. L.Nguyen, L.Hoang, P. Fine, Q.Tong, B. Ma, R. Humphreys, A. Savoca, C.P. Wong, S. Shi, M. Vincent, and L. Wang, *"High Performance Underfill Development –Materials, Processes, and Reliability."* In Proc. 1st IEEE Int. Symp. Polymeric Electron. Packag, Norrköping, Sweden, October 26-30, 1997, pp 300-306

[26] H.Peng, R.Wayne, G.Flowers. E.Yeager, M.Konarsk, A. Torres, L.Crane, *"Underfilling Micro-BGA's"*, Loctite Research, Development and Engineering, Loctite Technical Paper.
 http://www.loctite.com/electronics_html/underfilling_micro_bgas.pdf

[27] T. Trichy, P. Sandborn, R. Raghavan, and S. Sahasrabudhe, "A New Test/Diagnosis/Rework Model for Use in Technical Cost Modeling of Electronic Systems Assembly," Proc of Int. Test Conf., pp. 1108-1117, 2001.

[28] D. Becker and P. Sandborn, " On the Use of Yielded Cost in Modeling Electronic Assembly Processes," IEEE Trans. On Electronics Packaging Manufacturing, vol. 24, pp. 195-202, July 2001.

[29] J. Petek, H. Charles, "Known Good Die, Die Replacement (Rework) and Their Influences on Multichip Module Costs," 48th IEEE Electronic Components and Technology Conference, pp 909-915, 1998.

[30] T. W. Williams and N. C. Brown, *"Defect Level as a Function of Fault Coverage," IEEE Trans. On Comp.*, vol. C-30, no. 12, pp. 987-988, December 1981.

Ben Salomon